

000 001 002 003 004 005 006 007 008 009 010 011 012 013 014 015 016 017 018 019 020 021 022 023 024 025 026 027 028 029 030 031 032 033 034 035 036 037 038 039 040 041 042 043 044 045 046 047 048 049 050 051 052 053 TOOLWEAVER: WEAVING COLLABORATIVE SEMANTICS FOR SCALABLE TOOL USE IN LARGE LANGUAGE MODELS

Anonymous authors

Paper under double-blind review

ABSTRACT

Prevalent retrieval-based tool-use pipelines struggle with a dual semantic challenge: their retrievers often employ encoders that fail to capture complex semantics, while the Large Language Model (LLM) itself lacks intrinsic tool knowledge from its natural language pretraining. Generative methods offer a powerful alternative by unifying selection and execution, tasking the LLM to directly learn and generate tool identifiers. However, the common practice of mapping each tool to a unique new token introduces substantial limitations: it creates a scalability and generalization crisis, as the vocabulary size explodes and each tool is assigned a semantically isolated token. This approach also creates a semantic bottleneck that hinders the learning of collaborative tool relationships, as the model must infer them from sparse co-occurrences of monolithic tool IDs within a vast library. To address these limitations, we propose **ToolWeaver**, a novel generative tool learning framework that encodes tools into hierarchical sequences. This approach makes vocabulary expansion logarithmic to the number of tools. Crucially, it enables the model to learn collaborative patterns from the dense co-occurrence of shared codes, rather than the sparse co-occurrence of monolithic tool IDs. We generate these structured codes through a novel tokenization process designed to weave together a tool’s intrinsic semantics with its extrinsic co-usage patterns. These structured codes are then integrated into the LLM through a generative alignment stage, where the model is fine-tuned to produce the hierarchical code sequences. Evaluation results with nearly 47,000 tools show that **ToolWeaver** significantly outperforms state-of-the-art methods, establishing a more scalable, generalizable, and semantically-aware foundation for advanced tool-augmented agents.

1 INTRODUCTION

LLMs have rapidly evolved into powerful interactive agents by integrating with external tools, enabling them to access dynamic information and perform comprehensive real-world tasks (Yao et al., 2023; Qin et al., 2023; Wang et al., 2024b; Hao et al., 2023; Zhao et al., 2025). Concurrently, the number and diversity of available tools have grown substantially, ranging from general services to domain-specific APIs, leading to significant challenges such as scalability and generalization for tool selection and execution (Mialon et al., 2023).

Existing methods (Patil et al., 2023; Wang et al., 2024b; Hao et al., 2023; Qin et al., 2024; Paranjape et al., 2023; Yao et al., 2023) have focused on equipping LLMs with tool-use capabilities through retrieval-based or generative approaches. Retrieval-based methods, such as ToolLLM (Qin et al., 2023) and Gorilla (Patil et al., 2023), employ external retrievers to select tools from a large corpus, which are often constrained by the LLM’s input length and add pipeline complexity. In contrast, generative methods (Wang et al., 2024b; Hao et al., 2023) offer end-to-end simplicity by fine-tuning the LLM to directly generate tool invocations. A common strategy in this paradigm is to map each tool to a unique special token (Liu et al., 2024).

However, this simple “one-token-per-tool” paradigm suffers from two fundamental drawbacks. Firstly, it faces a **critical scalability and generalization challenge**. As illustrated in Figure 1(a), the

vocabulary size grows linearly with the number of tools, which hinders generalization as each new tool requires a semantically isolated token. For a model like Llama-3-8B (Dubey et al., 2024) with a vocabulary of 128,256, integrating a large benchmark like ToolBench would require adding nearly 47,000 new tokens. This massive injection of out-of-vocabulary (OOV) tokens leads to significant memory overhead and risks disrupting the model’s pretrained linguistic knowledge, causing a catastrophic degradation of its general language capabilities (Wang et al., 2024a). Secondly, it suffers a **semantic bottleneck for complex reasoning**. By flattening tools into isolated, unique tokens, the model struggles to learn collaborative relationships, as it is forced to rely on the statistically sparse co-occurrence of their individual IDs. For instance, consider the query “is it a good day to take my kid to the park?” as illustrated in Figure 1(b). To answer this comprehensively, a model needs to infer the relationship between tools like Realtime Weather and Air Quality. However, because the joint appearance of any specific tool pair is rare in a vast library, the model might check the weather but fail to consider air quality, thus providing an incomplete or misleading answer.

To address these challenges, we propose ToolWeaver, a framework that fundamentally rethinks tool representation. Instead of flat identifiers, ToolWeaver represents each tool as a compositional sequence of discrete codes. This hierarchical structure, generated via our novel, unsupervised collaborative-aware vector quantization, is not only highly scalable—reducing vocabulary expansion from linear to logarithmic—but more importantly, it is inherently compatible with the autoregressive nature of LLMs and enables the model to learn from a dense collaborative signal.

By jointly modeling a tool’s intrinsic function and its extrinsic co-usage patterns, this method encourages functionally related tools to share codes. For instance, Realtime Weather (<T1_1><T2_1>) and Air Quality (<T1_1><T2_2>) can share a parent code (<T1_1>) that emerges to group tools for a shared context like “outdoor conditions”, allowing the model to learn their collaborative nature from the dense co-occurrence of the shared code rather than the sparse co-occurrence of individual tools. Subsequently, these structured codes are integrated into the LLM via a generative alignment stage, training the model to produce the hierarchical code sequences for complex tool invocation. In summary, our main contributions are as follows:

- We propose ToolWeaver, a novel framework that represents tools as compositional codes. A collaborative-aware tokenization process generates these codes, enabling the model to learn robust collaborative patterns from the dense co-occurrence of shared codes, thus overcoming the scalability and semantic bottlenecks of prior methods while enhancing generalization.
- We introduce a multi-stage generative alignment process that effectively aligns the structured tool codes with the LLM’s internal knowledge. This fine-tuning teaches the model to natively generate the hierarchical code sequences, enabling both accurate tool selection and complex external tool use.
- Experimental validation on a large benchmark of nearly 47,000 tools demonstrates that ToolWeaver significantly outperforms state-of-the-art methods in complex task completion while substantially mitigating the impact on the LLM’s general capabilities.

2 RELATED WORK

2.1 LARGE LANGUAGE MODELS WITH TOOLS

Equipping LLMs with external tools (e.g., APIs, knowledge bases) enables them to execute complex, interactive tasks. Current methods are broadly categorized as tuning-free or tuning-based. Tuning-free approaches use in-context learning, placing tool descriptions and examples in the prompt to guide the LLM without updating its parameters (Qin et al., 2024; Paranjape et al., 2023; Yao et al., 2023; Wu et al., 2024; Liu et al., 2025). In contrast, tuning-based methods fine-tune LLMs on tool-use datasets (Schick et al., 2023; Wang et al., 2024b). This has evolved from domain-specific tools like retrieval modules (Gao et al., 2024b) (e.g., WebGPT (Nakano et al., 2022) for web browsing (Brown et al., 2020)) to general-purpose toolsets (Qin et al., 2023; Li et al., 2023) (e.g., Toolformer (Schick et al., 2023) using calculators, QA systems) (Zhuang et al., 2023; Chen et al., 2025).

The growing scale of toolsets, highlighted by benchmarks like ToolBench (Qin et al., 2023) and API-Bank (Li et al., 2023), creates a major scalability problem. In-context methods face context

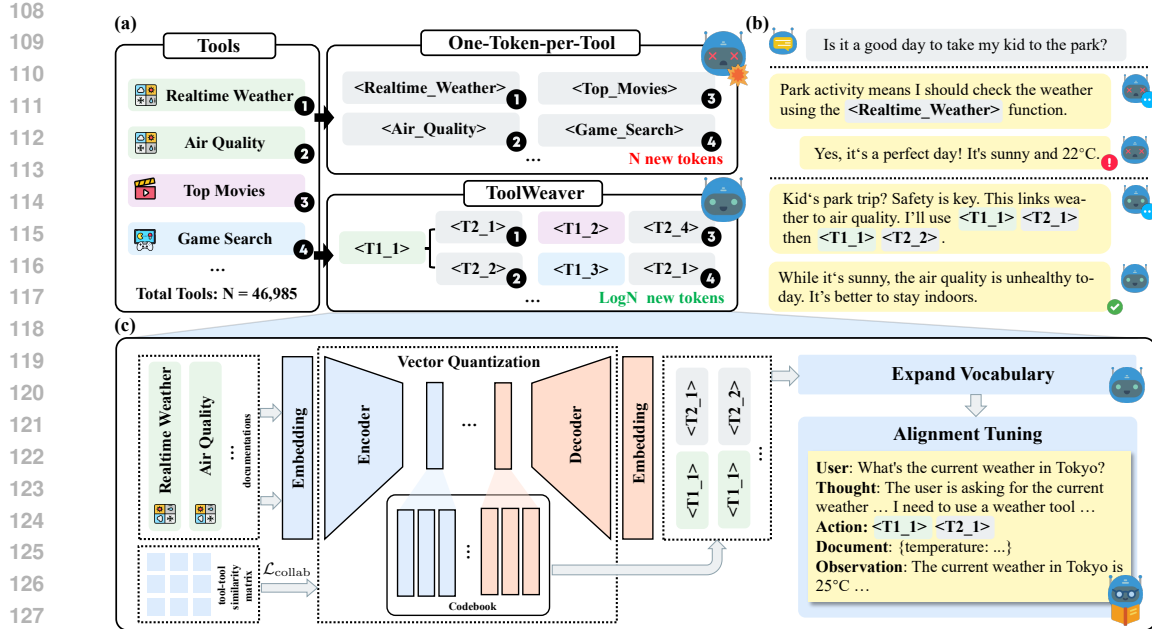


Figure 1: An overview of the ToolWeaver framework. (a) We contrast the standard “one-token-per-tool” method, which creates a massive flat vocabulary, with our compositional approach that scales logarithmically. (b) Our model leverages collaborative signals between tools (e.g., *Realtime Weather* and *Air Quality*) for complex reasoning where “one-token-per-tool” representations fail. (c) The ToolWeaver architecture learns these structured representations through a collaborative-aware vector quantization process, which are then integrated into an LLM.

window limitations, while tuning-based methods require constant retraining. This necessitates more efficient tool retrieval and selection mechanisms.

2.2 TOOL SELECTION

With expanding toolkits, effective tool selection is critical. One approach is retriever-based selection, which treats tools as documents to be ranked by information retrieval models like BM25 (Robertson & Zaragoza, 2009) or dense retrievers (Karpukhin et al., 2020; Xiong et al., 2020), as used in Gorilla (Patil et al., 2023). While techniques like query rewriting (Chen et al., 2024) and iterative refinement (Xu et al., 2024) improve accuracy, these pipelines suffer from high latency and complexity.

An alternative is generative selection, where each tool is mapped to a single, atomic token that the LLM generates directly (Hao et al., 2023; Wang et al., 2024b). ToolGen (Wang et al., 2024b) exemplifies this by integrating tool knowledge as virtual tokens. However, this approach scales poorly: large tool vocabularies increase memory and latency, artificial tokens can disrupt linguistic priors, and the flat token representation impedes reasoning over semantic tool relationships.

2.3 INTEGRATING COLLABORATIVE SEMANTICS INTO LLMs

Recent research seeks to integrate collaborative semantics into LLMs, bridging the semantic gap between their native linguistic space and the symbolic knowledge embedded in collaborative signals (Lin et al., 2025). Existing methods primarily project collaborative knowledge into the LLM’s semantic space. For instance, SeLLa-Rec (Wang et al., 2025) maps collaborative knowledge to specialized tokens, while LC-Rec (Zheng et al., 2024) utilizes learning-based vector quantization via a Residual-Quantized Variational AutoEncoder (RQ-VAE) (Lee et al., 2022) to generate structured identifiers. Others leverage graph structures, such as GAL-Rec (Guan et al., 2024), which uses GNN-inspired techniques to teach relational patterns. This principle also extends to generative retrieval, where models like CFRAG (Shi et al., 2025) infuse collaborative filtering into the RAG pipeline.

162 Despite their progress, these approaches share a fundamental limitation: they all rely on post-hoc
 163 alignment. This paradigm introduces semantically isolated identifiers and then forces the model to
 164 learn their meaning through a separate alignment phase, disconnected from its foundational rep-
 165 resentations. This reveals a critical research gap for a more foundational approach that integrates
 166 collaborative semantics directly into the tokenization process, enriching representations from the
 167 ground up.

168

169 3 TOOLWEAVER

170

171 3.1 PRELIMINARIES

172

173 Current tool-augmented agents often operate by iteratively reasoning and acting. Given a user query
 174 q and a large tool corpus $\mathcal{D} = \{d_1, \dots, d_N\}$ where $|\mathcal{D}| = N$, an agent typically follows a multi-stage
 175 process: (1) planning a step (p_i), (2) selecting a tool (d_i), (3) generating its parameters (α_i), and (4)
 176 observing the execution feedback (f_i). This cycle repeats until the task is complete, forming an
 177 interaction trajectory $\text{Traj} = [q, (p_1, d_1, \alpha_1, f_1), \dots, (p_t, d_t, \alpha_t, f_t), a]$. To streamline this process,
 178 a promising generative paradigm (Hao et al., 2023; Wang et al., 2024b) reframes tool selection as
 179 a next-token prediction task. This is achieved by mapping each tool $d \in \mathcal{D}$ to a unique, specially
 180 added token in the language model’s vocabulary. While simple, this “one-token-per-tool” scheme
 181 suffers from the scalability, generalization, and semantic limitations discussed in the introduction.

182

183 To overcome these challenges, we propose ToolWeaver. Instead of a single token, it represents each
 184 tool as a compositional sequence of discrete codes. As visualized in Figure 1(c), we employ a set of
 185 L codebooks, $\mathcal{C} = \{\mathcal{C}_1, \dots, \mathcal{C}_L\}$, where each codebook \mathcal{C}_l contains K learnable code vectors. Each
 186 tool is then mapped to a unique sequence of L indices, $[\iota_1, \iota_2, \dots, \iota_L]$. This hierarchical structure
 187 yields a representation capacity of up to K^L tools while only requiring the addition of $L \times K$ new
 188 tokens to the vocabulary, achieving the logarithmic compression contrasted in Figure 1(a).

189

190 While this compositional structure is inherently scalable, the key contribution of ToolWeaver is
 191 its novel structured tokenization process. An integral aspect of this process is the explicit use of
 192 collaborative signals from tool usage data during codebook learning, which ensures the resulting
 193 representations are not only semantically coherent but also aligned with their practical, collaborative
 194 functions in downstream tasks.

195

196 3.2 STRUCTURED TOKENIZATION GUIDED BY COLLABORATIVE SEMANTICS

197

198 The core of ToolWeaver is its structured tokenization process (see Figure 1(c)), which transforms
 199 each tool’s unstructured documentation into a compositional representation. This process is de-
 200 signed to embed both semantic and collaborative relationships directly into the code structure. It
 201 involves a multi-stage pipeline of initial semantic encoding, collaborative-aware residual quantiza-
 202 tion, and conflict mitigation.

203

204 **Initial Semantic Representation.** Given the textual documentation for each tool $d \in \mathcal{D}$ (including
 205 its name and description), we first leverage a powerful pretrained text encoder to generate a dense
 206 semantic embedding. This initial representation, denoted as $e_d \in \mathbb{R}^D$, captures the core functionality
 207 of the tool.

208

$$e_d = \text{Text-Encoder}(\text{Doc}_d), \quad (1)$$

209 these embeddings $\{e_d\}_{d \in \mathcal{D}}$ serve as the foundational input for our structured tokenization frame-
 210 work.

211

212 **Collaborative-Aware Residual Quantization.** To create a compact and hierarchical code struc-
 213 ture, we employ an RQ-VAE (Lee et al., 2022), a multi-level vector quantization approach. This
 214 method operates without requiring human-annotated labels. Unlike traditional single-layer vec-
 215 tor quantization or simple clustering algorithms that offer a flat representation, RQ-VAE sequen-
 216 tially quantizes residual errors, allowing it to achieve a significantly larger expression space with
 217 a more compact and manageable vocabulary size. As defined in the preliminaries, we use L code-
 218 books, $\{\mathcal{C}_1, \dots, \mathcal{C}_L\}$, where each codebook \mathcal{C}_l contains K learnable centroid vectors $\{v_{l,k}\}_{k=1}^K$, with
 219 $v_{l,k} \in \mathbb{R}^{D'}$. For efficiency, we first reduce the dimensionality of the initial embeddings e_d from D
 220 to D' using a linear projection, yielding z_d .

216 The quantization process is recursive. For each tool d , the initial residual is set to its projected
 217 embedding, $r_{d,1} = z_d$. At each level $l \in \{1, \dots, L\}$, we find the closest centroid in codebook \mathcal{C}_l for
 218 the current residual $r_{d,l}$ and subtract it to compute the residual for the next level:
 219

$$220 \quad \iota_{d,l} = \arg \min_{k \in \{1, \dots, K\}} \|r_{d,l} - v_{l,k}\|_2^2, \quad (2)$$

$$222 \quad r_{d,l+1} = r_{d,l} - v_{l,\iota_{d,l}}, \quad (3)$$

223 where $\iota_{d,l}$ is the discrete code index assigned to tool d at level l . The final quantized representation
 224 is the sum of the selected codebook vectors: $\hat{z}_d = \sum_{l=1}^L v_{l,\iota_{d,l}}$.
 225

226 The standard RQ-VAE is trained to minimize a combination of a reconstruction loss and a quantiza-
 227 tion loss:
 228

$$229 \quad \mathcal{L}_{\text{recon}} = \|z_d - \hat{z}_d\|_2^2, \quad (4)$$

$$230 \quad \mathcal{L}_{\text{quant}} = \sum_{l=1}^L (\|\text{sg}[r_{d,l}] - v_{l,\iota_{d,l}}\|_2^2 + \beta \|r_{d,l} - \text{sg}[v_{l,\iota_{d,l}}]\|_2^2).$$

233 where $\text{sg}[\cdot]$ is the stop-gradient operator and β is a commitment weight, typically set to 0.25.
 234

235 To ensure the resulting codes capture not only a tool’s intrinsic function but also its extrinsic collab-
 236 orative patterns, we guide the quantization process using a pre-computed tool-tool similarity matrix
 237 A .
 238

239 This matrix is derived from a tool co-occurrence matrix C built from the usage trajectories, where
 240 each element C_{uv} counts the total number of times tools u and v appear together. The similarity
 241 score A_{uv} is then calculated using cosine similarity:
 242

$$243 \quad A_{uv} = \frac{C_{uv}}{\sqrt{C_{uu} \cdot C_{vv}}}, \quad (5)$$

244 where C_{uu} and C_{vv} represent the total occurrence counts for tools u and v , respectively.
 245

246 We introduce a graph Laplacian regularization term that encourages similar tools to have nearby
 247 quantized representations:
 248

$$249 \quad \mathcal{L}_{\text{collab}} = \sum_{u,v \in \mathcal{D}} A_{uv} \|\hat{z}_u - \hat{z}_v\|_2^2. \quad (6)$$

250 This term penalizes large distances between the quantized representations of tools that frequently
 251 co-occur or are functionally related. This integration with RQ is crucial, as its multi-layer, residual
 252 nature facilitates a progressive refinement of collaborative semantics: the initial layers capture broad
 253 functional similarities, while subsequent layers model finer distinctions on the residual information.
 254 Combining these objectives, the final training objective for our structured tokenization becomes:
 255

$$256 \quad \mathcal{L}_{\text{tokenize}} = \mathbb{E}_{d \sim \mathcal{D}} [\mathcal{L}_{\text{recon}} + \mathcal{L}_{\text{quant}}] + \lambda \mathcal{L}_{\text{collab}}, \quad (7)$$

257 where λ is a hyperparameter balancing the reconstruction fidelity with the collaborative structure
 258 alignment.
 259

260 **Conflict Mitigation via Uniform Mapping.** A practical challenge in any tree-based or multi-level
 261 quantization is index collision, where multiple distinct tools map to the exact same sequence of code
 262 indices $[\iota_1, \dots, \iota_L]$. A naive solution of adding an extra, semantically meaningless layer of IDs
 263 is undesirable, as it can disrupt the learned semantic structure. To resolve this while preserving
 264 semantic integrity, we enforce a uniform mapping constraint on the final codebook \mathcal{C}_L .
 265

266 Our objective is to ensure that tool representations are distributed as uniformly as possible across the
 267 centroids of the final codebook. We formulate this as a constrained optimization problem, adapting
 268 the standard quantization objective for the final level L . For a batch of final-level residuals $\mathcal{B}_L =$
 269 $\{r_{d,L}\}_{d \in \text{batch}}$, we aim to solve:
 270

$$271 \quad \min_{\Pi} \sum_{d \in \mathcal{B}_L} \sum_{k=1}^K \pi_{dk} \|r_{d,L} - v_{L,k}\|_2^2, \quad (8)$$

270 subject to:

271
272
$$\forall d, \sum_{k=1}^K \pi_{dk} = 1, \forall k, \sum_{d \in \mathcal{B}_L} \pi_{dk} = \frac{|\mathcal{B}_L|}{K}, \quad (9)$$

273

274 where $\pi_{dk} = p(\iota_{d,L} = k | r_{d,L})$ represents the soft assignment probability of tool d 's residual to
275 centroid k . The first constraint ensures that each tool's residual is fully assigned across the codebook.
276 The second, more critical constraint, enforces that each centroid in the final codebook is assigned an
277 equal share of tools from the batch, thereby mitigating collisions.278 Following Zheng et al. (2024), we frame this as an optimal transport problem where $\|r_{d,L} - v_{L,k}\|^2$
279 is the transport cost. This formulation allows us to find an optimal assignment matrix Π that satisfies
280 the uniform distribution constraint. In our implementation, we solve this problem efficiently using
281 the Sinkhorn-Knopp algorithm (Cuturi, 2013). This strategy promotes a unique identifier for every
282 tool without compromising the learned semantic space.283
284 3.3 MULTI-STEP GENERATIVE ALIGNMENT TUNING
285286 The final stage of our framework is to integrate these structured codes into the LLM via generative
287 alignment tuning. The code sequence for each tool, e.g., $[\iota_{d,1}, \dots, \iota_{d,L}]$, is mapped to a sequence
288 of new, unique tokens (e.g., $\langle T1_1 \rangle \langle T2_1 \rangle$) added to the LLM's vocabulary. Let ι_d denote this
289 sequence of code-tokens. The corresponding embeddings for these new vocabulary tokens are ran-
290 domly initialized. We then fine-tune the model in two stages:291
292 **Stage 1: Tool Retrieval Alignment.** The model learns to generate the correct tool's code sequence
293 ι_d from a user query q by fine-tuning on a dataset of query-tool pairs.

294
$$\mathcal{L}_{\text{retrieval}} = -\mathbb{E}_{(q,d)}[\log P(\iota_d|q)]. \quad (10)$$

295

296 **Stage 2: Tool Usage Trajectory Alignment.** We further fine-tune the model on full interaction
297 trajectories. The model learns to generate sequences of reasoning, actions (tool calls, including
298 their code-tokens ι_d and parameters α_d), and final answers, with the loss computed only over the
299 assistant's tokens.300 This progressive tuning aligns the model for both accurate tool selection and effective execution in
301 downstream tasks.302
303 3.4 INFERENCE
304305 To prevent the model from generating invalid tool codes during inference, we employ a constrained
306 beam search, a standard technique in similar generative frameworks (Wang et al., 2024b). A pre-
307 computed prefix tree (trie) of all valid tool code sequences (ι_d for all $d \in \mathcal{D}$) guides the search,
308 ensuring that only valid identifiers are generated by masking the logits of invalid next tokens at each
309 step. This constraint is applied only during the tool selection phase, preserving the model's full
310 generative capacity for other tasks.311
312 4 EXPERIMENTS
313314 We conduct extensive experiments to evaluate ToolWeaver on large-scale tool retrieval and end-
315 to-end evaluation, focusing on performance, generalization, and scalability against state-of-the-art
316 methods.317
318 4.1 EXPERIMENTAL SETUP319 **Dataset.** We use the large-scale ToolBench benchmark (Qin et al., 2023), which consists of over
320 16,000 tool collections comprising 46,985 unique APIs. Although a tool collection may contain
321 multiple APIs, for simplicity, we refer to each individual API as a “tool” in this paper.322 The dataset's structure allows evaluation across scenarios of increasing complexity, from simple
323 single-tool tasks (I1), to multi-tool planning within a single category (I2), and finally to complex

orchestration of tools across different categories (I3) (Qin et al., 2023). Furthermore, to rigorously assess generalization, we adopt fine-grained splits: I1 Tool., I1 Cat., and I2 Cat., where “Tool.” and “Cat.” denote tools and categories, respectively, that are unseen during training. All data for our retrieval and agent-tuning experiments are converted from this benchmark, with further details in Appendix A.1.

Baselines. We compare ToolWeaver against a comprehensive set of baselines for both tool retrieval and end-to-end task completion. For retrieval evaluation, we use the classic unsupervised methods BM25 (Robertson & Zaragoza, 2009) and Embedding Similarity (EmbSim), alongside the state-of-the-art supervised models ToolRetriever (Qin et al., 2023) and ToolGen (Wang et al., 2024b). For end-to-end evaluation, we benchmark against strong generative models including GPT-4o-mini, ToolLlama-2 (Qin et al., 2023), and ToolGen (Wang et al., 2024b). A detailed description of each baseline is provided in Appendix A.2.

Metrics. For tool retrieval, we use Normalized Discounted Cumulative Gain (NDCG@k) (Järvelin & Kekäläinen, 2002) for $k=\{1,3,5\}$, which evaluates the ranking quality of retrieved tools by considering both relevance and position. For the agent task, we adopt the StableToolBench framework (Guo et al., 2024) and report two key metrics: Solvable Pass Rate (SoPR), the percentage of tasks successfully completed, and Solvable Win Rate (SoWR), which measures the quality of the final answer against a strong reference model.

Implementation Details. For our main experiments presented in the body of this paper, we use the pretrained Llama-3-8B as the primary foundation model for both ToolWeaver and key generative baselines to ensure a fair comparison. To demonstrate the robustness and generalizability of our approach across different architectures, we provide a full set of supplementary results using the Qwen model series (Yang et al., 2025) in Appendix B.3. All other architectural choices, training procedures, and hyperparameter settings are detailed in Appendix A.3.

Table 1: Tool retrieval evaluation performance on ToolBench. Performance is measured by NDCG@k across varying query complexities (I1-I3) and generalization settings (I1-Tool, I1-Cat, I2-Cat). ToolWeaver consistently outperforms both retrieval-based (BM25, EmbSim, ToolRetriever) and generative (ToolGen) methods.

Model	NDCG@1			NDCG@3			NDCG@5		
	I1	I2	I3	I1	I2	I3	I1	I2	I3
BM25	26.92	20.00	10.00	26.13	21.92	10.08	29.00	23.46	12.33
EmbSim	50.50	46.00	18.00	48.15	39.58	17.77	53.41	43.05	20.94
ToolRetriever	75.92	63.00	28.00	76.96	66.38	39.28	82.31	72.72	44.54
ToolGen	88.50	84.00	81.00	88.83	85.65	80.83	91.65	89.02	85.83
ToolWeaver	91.16	89.76	88.00	91.14	89.70	85.80	93.48	91.80	90.12
	I1-Tool.	I1-Cat.	I2-Cat.	I1-Tool.	I1-Cat.	I2-Cat.	I1-Tool.	I1-Cat.	I2-Cat.
BM25	20.75	20.63	16.58	21.12	20.67	19.55	23.64	24.18	20.89
EmbSim	53.00	58.00	35.68	49.82	54.38	33.92	54.93	52.94	36.22
ToolRetriever	75.25	73.50	60.30	78.26	73.56	64.11	83.08	79.10	73.01
ToolGen	84.00	89.50	83.42	86.40	89.95	86.06	89.52	90.01	88.47
ToolWeaver	86.50	92.50	89.45	88.44	90.75	88.19	90.72	92.30	89.85

4.2 RESULTS

Table 1 presents a comprehensive comparison of tool retrieval evaluation performance. Across all query complexities (I1-I3) and generalization settings (Tool./Cat.), ToolWeaver consistently outperforms all baselines. In the most complex I3 scenario, ToolWeaver achieves an NDCG@1 of 88.00, significantly higher than ToolGen (81.00) and all retrieval-based methods. This advantage holds in generalization tests; for instance, on the I1-Cat setting, ToolWeaver’s NDCG@5 score of 92.30 surpasses ToolGen’s 90.12, demonstrating robust semantic alignment and compositional generalization. Table 2 details the end-to-end evaluation results. ToolWeaver achieves superior performance in most cases, excelling in both task completion (SoPR) and solution quality (SoWR). In the challenging retrieval setting, ToolWeaver attains the highest SoPR scores in nearly all scenarios. Its

378
 379
 380
 381
 382
 383
 384
 385 Table 2: Comparison of end-to-end evaluation performance on ToolBench, measured by Solvable
 386 Pass Rate (SoPR) and Solvable Win Rate (SoWR). The SoWR is calculated against the GPT-4o-
 387 mini baseline. GPT-4o-mini and ToolLlama-2 are tested in a challenging Retrieval setting (Re.) that
 388 requires selecting tools from the full set. In contrast, ToolGen and ToolWeaver generate tool tokens
 389 directly, without the need for a retriever. ToolWeaver outperforms other models in diverse scenarios,
 390 highlighting its effectiveness in both tool selection and execution.

Model	Set.	SoPR						SoWR					
		I1	I2	I3	I1Tool.	I1Cat.	I2Cat.	I1	I2	I3	I1Tool.	I1Cat.	I2Cat.
GPT-4o-mini	Re.	52.25	40.41	24.86	53.16	50.11	39.38	-	-	-	-	-	-
ToolLlama-2	Re.	28.94	24.69	10.93	28.48	36.93	19.09	25.15	30.19	24.59	26.58	27.45	20.16
ToolGen		52.97	45.13	36.34	45.36	55.56	45.56	36.20	42.45	49.18	32.91	42.48	37.90
ToolWeaver		53.17	44.03	52.19	54.85	57.41	46.24	40.49	48.11	59.02	36.08	43.14	35.48

391 advantages are clear not only in simple (I1) and complex multi-tool tasks (I3), but also in gener-
 392 alizing to both unseen tools (I1-Tool) and unseen categories (I1-Cat). The substantial lead in the
 393 multi-tool I3 scenario (52.19 vs. ToolGen’s 36.34) particularly underscores the effectiveness of
 394 our collaborative-aware design for complex planning. Regarding SoWR against the GPT-4o-mini
 395 reference, ToolWeaver again demonstrates superior performance in the majority of scenarios. The
 396 advantage is particularly pronounced in the most complex I3 tasks, where it achieves a win rate
 397 of 59.02, substantially outperforming ToolGen (49.18). Full results across all settings, including
 398 additional baselines and evaluation domains, are detailed in Appendix B.1.

4.3 ABLATION STUDIES AND ANALYSIS

4.3.1 ANALYSIS OF COLLABORATIVE REGULARIZATION WEIGHT

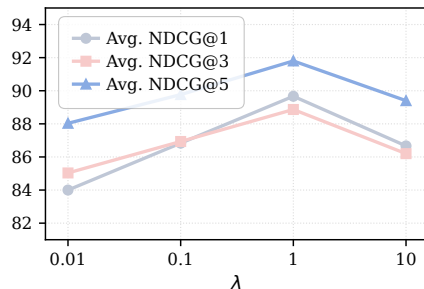
403 We conducted a sensitivity analysis to assess
 404 the impact of the collaborative regularization
 405 weight, λ , on tool selection performance. As
 406 shown in Figure 2, model performance across
 407 all NDCG metrics consistently improves as λ
 408 increases from 0.01 to 1, peaking at $\lambda=1$. This
 409 trend demonstrates that incorporating collabora-
 410 tive signals is crucial for learning a semanti-
 411 cally rich representation that captures how tools
 412 function together. However, when λ is in-
 413 creased further to 10, performance declines, in-
 414 dicating that an excessively strong collabora-
 415 tive prior can distort tool representations by sacri-
 416 ficing the fidelity of their intrinsic functions. This
 417 result empirically validates our central hypoth-
 418 esis: optimal performance is achieved by strik-
 419 ing a balance between a tool’s intrinsic seman-
 420 tics and its extrinsic collaborative patterns, con-
 421 firming the effectiveness of ToolWeaver’s design.

4.3.2 COMPONENT ABLATION ANALYSIS

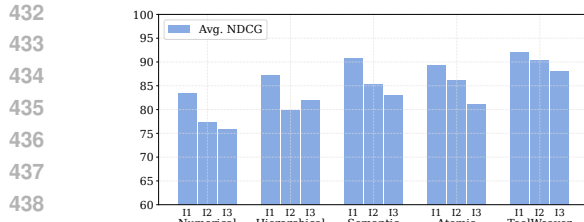
423 To demonstrate the cumulative impact of our core components, we performed a step-wise ablation.
 424 The results in Figure 3 reveal a clear hierarchy of contributions.

425 The model without semantic initialization (blue bars), which lacks both of our proposed compo-
 426 nents, performs poorly and serves as a baseline. The first crucial step is adding semantic initializa-
 427 tion. This step alone (transitioning from blue to pink bars) causes a dramatic performance leap of
 428 over 20 NDCG points, underscoring that a meaningful tool representation is the single most critical
 429 foundation.

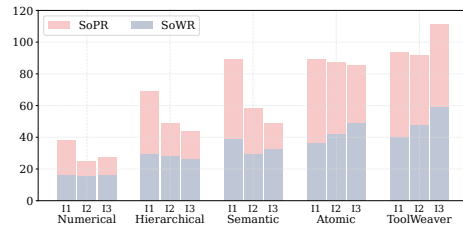
430 Building upon this semantically-aware foundation, the final step is to incorporate collaborative guid-
 431 ance (transitioning from pink to grey bars). This yields a further, significant improvement whose



432 Figure 2: Analysis of the collaborative regulariza-
 433 tion weight λ . Performance, measured by average
 434 NDCG@k across all I1-I3 scenarios, consistently
 435 peaks at $\lambda = 1$.



(a) Retrieval Evaluation (Avg. NDCG@{1,3,5}).



(b) End-to-end Evaluation (SoPR/SoWR).

Figure 4: Comparison of tokenization strategies.

magnitude scales with task complexity. The benefit is modest for simple I1 tasks but becomes most pronounced for complex, multi-tool I3 tasks. This trend provides strong evidence for our thesis: while semantic understanding is foundational, explicitly encoding collaborative patterns is the key to mastering complex tool orchestration.

4.3.3 COMPARISON OF TOKENIZATION STRATEGIES

To further validate the effectiveness of our collaborative-aware structured tokenization, particularly against other methods that attempt to embed structure or semantics into tool representations, we compare ToolWeaver against several alternative strategies. These baselines represent different paradigms: **Atomic** (as in ToolGen) assigns a single unique token per tool, serving as a flat generative baseline; **Numerical** uses fixed-length numeric strings, providing a minimal-vocabulary but non-semantic baseline; **Hierarchical** generates structured code sequences based on clustering, representing a static, tree-like approach to tokenization; and **Semantic** leverages human-readable parts of tool names, reflecting a direct, lexicon-based semantic approach. Detailed descriptions of these methods are provided in Appendix B.2.

As shown in Figure 4, ToolWeaver consistently outperforms all other tokenization strategies across both tool retrieval and end-to-end evaluation. Notably, while the Hierarchical and Semantic methods attempt to incorporate structure, they struggle to outperform the strong Atomic baseline, particularly in the end-to-end evaluation (SoPR/SoWR). This indicates that simply adding a naive structure is not sufficient for improving performance.

These results underscore the core advantage of ToolWeaver: it does not merely rely on pre-existing hierarchies or basic semantic similarity. Instead, it uniquely weaves collaborative signals into a structured, semantic representation. The underperformance of other structured methods compared to the Atomic baseline highlights that the quality and type of encoded information are critical. ToolWeaver’s holistic approach creates tool codes that are not only descriptive of a tool’s function but also predictive of its role in complex, multi-tool workflows, leading to superior performance.

4.3.4 IMPACT ON GENERAL LANGUAGE CAPABILITIES

A critical concern with generative tool learning is that adding new tokens might disrupt the pre-trained linguistic knowledge of the LLM. Methods like ToolGen inject nearly 47,000 new tokens, linearly expanding the vocabulary and potentially skewing the model’s internal distribution. In contrast, ToolWeaver employs a logarithmic expansion strategy that adds significantly fewer tokens.

486 To rigorously quantify this impact, we selected two complementary evaluation protocols. First,
 487 we measured Perplexity (PPL) on WikiText-2 (Merity et al., 2016) to assess how well the model
 488 maintains the original probability distribution of natural language. Second, we evaluated Text Sum-
 489 marization on CNN/DailyMail (See et al., 2017) and XSum (Narayan et al., 2018) to verify the
 490 model’s ability to generate coherent and high-quality text in zero-shot settings.

491
 492 **Table 3: Impact of tool vocabulary expansion on general language capabilities.** We report Perplexity
 493 (lower is better) and Summarization BERTScore F1 (higher is better). ToolWeaver preserves the
 494 base model’s capabilities significantly better than ToolGen.

Model	Language Modeling (PPL)		Text Summarization (BERTScore F1)		
	WikiText-2 (↓)	CNN/DM (↑)	XSum (↑)	Avg. Drop	
Llama-3-8B (Base)	6.34	85.35	85.05	-	
ToolGen	104.54	82.93	82.53	2.47	
ToolWeaver	25.36	85.07	84.18	0.57	

501
 502 Table 3 summarizes the results. The linear vocabulary expansion in ToolGen leads to catastrophic
 503 degradation. Specifically, its PPL on WikiText-2 increases drastically to 104.54, which is approx-
 504 imately 16 times that of the base model. Furthermore, its generation quality drops notably on the
 505 abstractive XSum benchmark. In contrast, ToolWeaver demonstrates superior robustness. The PPL
 506 remains much lower at 25.36, and the summarization performance on CNN/DailyMail is nearly
 507 identical to the base model, achieving a BERTScore of 85.07 compared to the original 85.35.

508 These findings indicate that our structured tokenization preserves the linguistic core of the LLM
 509 far better than assigning isolated atomic tokens to a vast tool library. We provide additional eval-
 510 uations on general understanding benchmarks, such as MMLU, along with detailed experimental
 511 configurations in Appendix B.4.

5 CONCLUSION

515 In this paper, we introduced ToolWeaver, a framework designed to address the critical scalabil-
 516 ity, generalization, and semantic challenges of the “one-token-per-tool” paradigm. ToolWeaver
 517 represents each tool as a hierarchical sequence of discrete codes, making vocabulary expansion
 518 logarithmic to the number of tools. Through a novel, collaborative-aware tokenization process,
 519 our framework weaves a tool’s intrinsic semantics with its extrinsic co-usage patterns, encouraging
 520 functionally related tools to share codes. This allows the model to learn robust collaborative pat-
 521 terns from the dense co-occurrence of shared codes, rather than the sparse co-occurrence of isolated
 522 tool IDs. Extensive experiments on the ToolBench benchmark demonstrate that ToolWeaver signif-
 523 icantly outperforms state-of-the-art methods in complex task completion and generalization, while
 524 better preserving the model’s general language capabilities. Our work establishes a more scalable,
 525 generalizable, and semantically-aware foundation for building advanced tool-using agents, with fu-
 526 ture directions including reinforcement learning to autonomously discover collaborative patterns.

540 ETHICS STATEMENT
541

542 Our work aims to advance the capabilities of tool-using AI agents. We acknowledge the potential for
543 misuse, as more capable agents could be directed to interact with malicious APIs. Furthermore, the
544 ToolBench dataset, while based on real-world tools, was not audited for biases or privacy risks. We
545 present this as foundational research and emphasize that any real-world deployment requires robust
546 safety protocols and human oversight.

548 REPRODUCIBILITY STATEMENT
549

550 To ensure reproducibility, our complete source code is provided in the supplementary material. All
551 experimental configurations, including dataset processing (Appendix A.1), baseline details (Ap-
552 pendix A.2), and implementation hyperparameters (Appendix A.3), are thoroughly documented.
553 Our experiments utilize the public ToolBench dataset and the StableToolBench evaluation frame-
554 work.

556 REFERENCES
557

558 Yonatan Bisk, Rowan Zellers, Ronan Le Bras, Jianfeng Gao, and Yejin Choi. PIQA: Reasoning
559 about physical commonsense in natural language. In *Proc. of the AAAI Conf. on Artificial Intelli-
560 gence (AAAI)*, pp. 7432–7439. AAAI Press, 2020. doi: 10.1609/AAAI.V34I05.6239.

561 Tom B. Brown, Benjamin Mann, Nick Ryder, Melanie Subbiah, Jared Kaplan, Prafulla Dhari-
562 wal, Arvind Neelakantan, Pranav Shyam, Girish Sastry, Amanda Askell, Sandhini Agarwal,
563 Ariel Herbert-Voss, Gretchen Krueger, Tom Henighan, Rewon Child, Aditya Ramesh, Daniel M.
564 Ziegler, Jeffrey Wu, Clemens Winter, Christopher Hesse, Mark Chen, Eric Sigler, Mateusz Litwin,
565 Scott Gray, Benjamin Chess, Jack Clark, Christopher Berner, Sam McCandlish, Alec Radford,
566 Ilya Sutskever, and Dario Amodei. Language models are few-shot learners, 2020.

567 Sijia Chen, Yibo Wang, Yi-Feng Wu, Qing-Guo Chen, Zhao Xu, Weihua Luo, Kaifu Zhang, and
568 Lijun Zhang. Advancing tool-augmented large language models: Integrating insights from errors
569 in inference trees, 2025.

571 Yanfei Chen, Jinsung Yoon, Devendra Singh Sachan, Qingze Wang, Vincent Cohen-Addad, Mo-
572 hammadhossein Bateni, Chen-Yu Lee, and Tomas Pfister. Re-Invoke: Tool invocation rewriting
573 for zero-shot tool retrieval, 2024.

575 Christopher Clark, Kenton Lee, Ming-Wei Chang, Tom Kwiatkowski, Michael Collins, and Kristina
576 Toutanova. BoolQ: Exploring the surprising difficulty of natural yes/no questions. In Jill Burstein,
577 Christy Doran, and Thamar Solorio (eds.), *Proc. of the Conf. of the North American Chapter of
578 the Association for Computational Linguistics (NAACL-HLT)*, pp. 2924–2936. Association for
579 Computational Linguistics, 2019. doi: 10.18653/V1/N19-1300.

580 Marco Cuturi. Sinkhorn distances: Lightspeed computation of optimal transport. *Advances in
581 Neural Information Processing Systems*, 26, 2013.

583 Abhimanyu Dubey, Abhinav Jauhri, Abhinav Pandey, Abhishek Kadian, Ahmad Al-Dahle, Aiesha
584 Letman, Akhil Mathur, Alan Schelten, Amy Yang, Angela Fan, et al. The Llama 3 herd of models,
585 2024.

586 Leo Gao, Jonathan Tow, Baber Abbasi, Stella Biderman, Sid Black, Anthony DiPofi, Charles Fos-
587 ter, Laurence Golding, Jeffrey Hsu, Alain Le Noac'h, Haonan Li, Kyle McDonell, Niklas Muen-
588 nighoff, Chris Ociepa, Jason Phang, Laria Reynolds, Hailey Schoelkopf, Aviya Skowron, Lintang
589 Sutawika, Eric Tang, Anish Thite, Ben Wang, Kevin Wang, and Andy Zou. The language model
590 evaluation harness, 07 2024a. URL <https://zenodo.org/records/12608602>.

592 Yunfan Gao, Yun Xiong, Xinyu Gao, Kangxiang Jia, Jinliu Pan, Yuxi Bi, Yi Dai, Jiawei Sun, Meng
593 Wang, and Haofen Wang. Retrieval-augmented generation for large language models: A survey,
2024b.

594 Zhong Guan, Likang Wu, Hongke Zhao, Ming He, and Jianpin Fan. Enhancing collaborative se-
 595 mantics of language model-driven recommendations via graph-aware learning, 2024.
 596

597 Zhicheng Guo, Sijie Cheng, Hao Wang, Shihao Liang, Yujia Qin, Peng Li, Zhiyuan Liu, Maosong
 598 Sun, and Yang Liu. StableToolBench: Towards stable large-scale benchmarking on tool learning
 599 of large language models, 2024.

600 Shibo Hao, Tianyang Liu, Zhen Wang, and Zhiting Hu. Toolkengpt: Augmenting frozen language
 601 models with massive tools via tool embeddings. *Advances in Neural Information Processing
 602 Systems*, 36:45870–45894, 2023.

603

604 Dan Hendrycks, Collin Burns, Steven Basart, Andy Zou, Mantas Mazeika, Dawn Song, and Jacob
 605 Steinhardt. Measuring massive multitask language understanding. In *Proc. of the Int. Conf. on
 606 Learning Representations (ICLR)*, 2021. URL <https://openreview.net/forum?id=d7KBjmI3GmQ>.

607

608 Kalervo Järvelin and Jaana Kekäläinen. Cumulated gain-based evaluation of IR techniques. *ACM
 609 Transactions on Information Systems (TOIS)*, 20(4):422–446, 2002.

610

611 Vladimir Karpukhin, Barlas Oğuz, Sewon Min, Patrick Lewis, Ledell Wu, Sergey Edunov, Danqi
 612 Chen, and Wen tau Yih. Dense passage retrieval for open-domain question answering, 2020.

613

614 Doyup Lee, Chiheon Kim, Saehoon Kim, Minsu Cho, and Wook-Shin Han. Autoregressive image
 615 generation using residual quantization. In *Proc. of the IEEE/CVF Conf. on Computer Vision and
 616 Pattern Recognition (CVPR)*, pp. 11523–11532, 2022.

617

618 Minghao Li, Yingxiu Zhao, Bowen Yu, Feifan Song, Hangyu Li, Haiyang Yu, Zhoujun Li, Fei
 619 Huang, and Yongbin Li. API-Bank: A comprehensive benchmark for tool-augmented LLMs,
 620 2023.

621

622 Jianghao Lin, Xinyi Dai, Yunjia Xi, Weiwen Liu, Bo Chen, Hao Zhang, Yong Liu, Chuhan Wu,
 623 Xiangyang Li, Chenxu Zhu, et al. How can recommender systems benefit from large language
 624 models: A survey. *ACM Transactions on Information Systems*, 43(2):1–47, 2025.

625

626 Qijiong Liu, Jieming Zhu, Yanting Yang, Quanyu Dai, Zhaocheng Du, Xiao-Ming Wu, Zhou Zhao,
 627 Rui Zhang, and Zhenhua Dong. Multimodal pretraining, adaptation, and generation for recom-
 628 mendation: A survey, 2024.

629

630 Yanming Liu, Xinyue Peng, Jiannan Cao, Shi Bo, Yuwei Zhang, Xuhong Zhang, Sheng Cheng, Xun
 631 Wang, Jianwei Yin, and Tianyu Du. Tool-Planner: Task planning with clusters across multiple
 632 tools, 2025.

633

634 Stephen Merity, Caiming Xiong, James Bradbury, and Richard Socher. Pointer sentinel mixture
 635 models, 2016.

636

637 Grégoire Mialon, Roberto Dessì, Maria Lomeli, Christoforos Nalmpantis, Ram Pasunuru, Roberta
 638 Raileanu, Baptiste Rozière, Timo Schick, Jane Dwivedi-Yu, Asli Celikyilmaz, Edouard Grave,
 639 Yann LeCun, and Thomas Scialom. Augmented language models: a survey, 2023.

640

641 Todor Mihaylov, Peter Clark, Tushar Khot, and Ashish Sabharwal. Can a suit of armor conduct
 642 electricity? a new dataset for open book question answering. In *Proc. of the Conf. on Empirical
 643 Methods in Natural Language Processing (EMNLP)*, 2018.

644

645 Reiichiro Nakano, Jacob Hilton, Suchir Balaji, Jeff Wu, Long Ouyang, Christina Kim, Christopher
 646 Hesse, Shantanu Jain, Vineet Kosaraju, William Saunders, Xu Jiang, Karl Cobbe, Tyna Eloun-
 647 dou, Gretchen Krueger, Kevin Button, Matthew Knight, Benjamin Chess, and John Schulman.
 648 WebGPT: Browser-assisted question-answering with human feedback, 2022.

649

650 Shashi Narayan, Shay B. Cohen, and Mirella Lapata. Don’t give me the details, just the summary!
 651 topic-aware convolutional neural networks for extreme summarization. *ArXiv*, abs/1808.08745,
 652 2018.

648 Bhargavi Paranjape, Scott Lundberg, Sameer Singh, Hannaneh Hajishirzi, Luke Zettlemoyer, and
 649 Marco Tulio Ribeiro. ART: Automatic multi-step reasoning and tool-use for large language mod-
 650 els, 2023.

651

652 Shishir G. Patil, Tianjun Zhang, Xin Wang, and Joseph E. Gonzalez. Gorilla: Large language model
 653 connected with massive APIs, 2023.

654

655 Yujia Qin, Shihao Liang, Yining Ye, Kunlun Zhu, Lan Yan, Yaxi Lu, Yankai Lin, Xin Cong, Xiangru
 656 Tang, Bill Qian, et al. Toolllm: Facilitating large language models to master 16000+ real-world
 657 APIs, 2023.

658 Yujia Qin, Shengding Hu, Yankai Lin, Weize Chen, Ning Ding, Ganqu Cui, Zheni Zeng, Yufei
 659 Huang, Chaojun Xiao, Chi Han, Yi Ren Fung, Yusheng Su, Huadong Wang, Cheng Qian, Runchu
 660 Tian, Kunlun Zhu, Shihao Liang, Xingyu Shen, Bokai Xu, Zhen Zhang, Yining Ye, Bowen Li,
 661 Ziwei Tang, Jing Yi, Yuzhang Zhu, Zhenning Dai, Lan Yan, Xin Cong, Yaxi Lu, Weilin Zhao,
 662 Yuxiang Huang, Junxi Yan, Xu Han, Xian Sun, Dahai Li, Jason Phang, Cheng Yang, Tongshuang
 663 Wu, Heng Ji, Zhiyuan Liu, and Maosong Sun. Tool learning with foundation models, 2024.

664

665 Stephen Robertson and Hugo Zaragoza. The probabilistic relevance framework: BM25 and beyond.
 666 *Foundations and Trends in Information Retrieval*, 3(4):333–389, 2009.

667

668 Keisuke Sakaguchi, Ronan Le Bras, Chandra Bhagavatula, and Yejin Choi. WinoGrande: An adver-
 669 sarial winograd schema challenge at scale. In *Proc. of the AAAI Conf. on Artificial Intelligence
 (AAAI)*, 2020.

670

671 Timo Schick, Jane Dwivedi-Yu, Roberto Dessì, Roberta Raileanu, Maria Lomeli, Luke Zettlemoyer,
 672 Nicola Cancedda, and Thomas Scialom. Toolformer: Language models can teach themselves to
 673 use tools, 2023.

674

675 Abigail See, Peter J. Liu, and Christopher D. Manning. Get to the point: Summarization with
 676 pointer-generator networks. In *Proceedings of the 55th Annual Meeting of the Association for
 677 Computational Linguistics (Volume 1: Long Papers)*, pp. 1073–1083, Vancouver, Canada, July
 678 2017. Association for Computational Linguistics. doi: 10.18653/v1/P17-1099. URL <https://www.aclweb.org/anthology/P17-1099>.

679

680 Teng Shi, Jun Xu, Xiao Zhang, Xiaoxue Zang, Kai Zheng, Yang Song, and Han Li. Retrieval
 681 augmented generation with collaborative filtering for personalized text generation. In *Proc. of the
 682 48th Int. ACM SIGIR Conf. on Research and Development in Information Retrieval (SIGIR)*, pp.
 683 1294–1304, 2025.

684

685 Liyuan Wang, Xingxing Zhang, Hang Su, and Jun Zhu. A comprehensive survey of continual
 686 learning: Theory, method and application. *IEEE Transactions on Pattern Analysis and Machine
 687 Intelligence*, 46(8):5362–5383, 2024a.

688

689 Renxi Wang, Xudong Han, Lei Ji, Shu Wang, Timothy Baldwin, and Haonan Li. Toolgen: Unified
 690 tool retrieval and calling via generation, 2024b.

691

692 Zihan Wang, Jinghao Lin, Xiaocui Yang, Yongkang Liu, Shi Feng, Daling Wang, and Yifei
 693 Zhang. Enhancing LLM-based recommendation through semantic-aligned collaborative knowl-
 694 edge, 2025.

695

696 Qinzhuo Wu, Wei Liu, Jian Luan, and Bin Wang. ToolPlanner: A tool augmented LLM for multi
 697 granularity instructions with path planning and feedback, 2024.

698

699 Lee Xiong, Chenyan Xiong, Ye Li, Kwok-Fung Tang, Jialin Liu, Paul Bennett, Junaid Ahmed,
 700 and Arnold Overwijk. Approximate nearest neighbor negative contrastive learning for dense text
 701 retrieval, 2020.

702 Qiancheng Xu, Yongqi Li, Heming Xia, and Wenjie Li. Enhancing tool retrieval with iterative
 703 feedback from large language models, 2024.

702 An Yang, Baosong Yang, Beichen Zhang, Binyuan Hui, Bo Zheng, Bowen Yu, Chengyuan Li,
 703 Dayiheng Liu, Fei Huang, Haoran Wei, Huan Lin, Jian Yang, Jianhong Tu, Jianwei Zhang, Jianxin
 704 Yang, Jiaxi Yang, Jingren Zhou, Junyang Lin, Kai Dang, Keming Lu, Keqin Bao, Kexin Yang,
 705 Le Yu, Mei Li, Mingfeng Xue, Pei Zhang, Qin Zhu, Rui Men, Runji Lin, Tianhao Li, Tianyi Tang,
 706 Tingyu Xia, Xingzhang Ren, Xuancheng Ren, Yang Fan, Yang Su, Yichang Zhang, Yu Wan,
 707 Yuqiong Liu, Zeyu Cui, Zhenru Zhang, and Zihan Qiu. Qwen2.5 technical report, 2025.

708 Shunyu Yao, Jeffrey Zhao, Dian Yu, Nan Du, Izhak Shafran, Karthik Narasimhan, and Yuan Cao.
 709 React: Synergizing reasoning and acting in language models. In *Proc. of the Int. Conf. on Learn-
 710 ing Representations (ICLR)*, 2023.

712 Rowan Zellers, Ari Holtzman, Yonatan Bisk, Ali Farhadi, and Yejin Choi. HellaSwag: Can a
 713 machine really finish your sentence? In *Proc. of the Annual Meeting of the Association for
 714 Computational Linguistics (ACL)*, 2019.

715 Wayne Xin Zhao, Kun Zhou, Junyi Li, Tianyi Tang, Xiaolei Wang, Yupeng Hou, Yingqian Min,
 716 Beichen Zhang, Junjie Zhang, Zican Dong, Yifan Du, Chen Yang, Yushuo Chen, Zhipeng Chen,
 717 Jinhao Jiang, Ruiyang Ren, Yifan Li, Xinyu Tang, Zikang Liu, Peiyu Liu, Jian-Yun Nie, and
 718 Ji-Rong Wen. A survey of large language models, 2025.

719 Bowen Zheng, Yupeng Hou, Hongyu Lu, Yu Chen, Wayne Xin Zhao, Ming Chen, and Ji-Rong Wen.
 720 Adapting large language models by integrating collaborative semantics for recommendation. In
 721 *Proc. of the IEEE 40th Int. Conf. on Data Engineering (ICDE)*, pp. 1435–1448. IEEE, 2024.

723 Yuchen Zhuang, Xiang Chen, Tong Yu, Saayan Mitra, Victor Bursztyn, Ryan A. Rossi, Somdeb
 724 Sarkhel, and Chao Zhang. ToolChain*: Efficient action space navigation in large language models
 725 with A* search, 2023.

726

727

728

729

730

731

732

733

734

735

736

737

738

739

740

741

742

743

744

745

746

747

748

749

750

751

752

753

754

755

APPENDIX

756	A Experimental Setup Details	15
761	A.1 Dataset Details	15
762	A.2 Baseline Details	16
764	A.3 Implementation and Training Details	17
765	A.4 Evaluation Setting Details	17
767	B Supplementary Experimental Results	18
769	B.1 Extended Results on Main Experiments	18
771	B.2 Detailed Comparison of Tokenization Strategies	19
772	B.3 Full Results on Qwen Models	20
774	B.4 Extended Analysis on General Language Capabilities	20
775	B.5 Codebook Hyperparameter Sensitivity Analysis	23
776	B.6 Sinkhorn-Knopp Efficiency and Stability Analysis	24
778	B.7 Inference Latency and Memory Analysis	25
779	B.8 Failure Analysis	27
781	C Qualitative Analysis and Examples	28
783	C.1 Case Study: Analysis of Learned Tool Codes and Multi-Tool Coordination	28
784	C.2 Examples for Tools and APIs	29
786	C.3 Examples of Alignment Tuning Data	29
787	C.4 Real End-to-End Inference Trajectory	29
789	D The Usage of LLMs	30

A EXPERIMENTAL SETUP DETAILS

A.1 DATASET DETAILS

Our experiments are conducted on the **ToolBench** benchmark (Qin et al., 2023), a large-scale and comprehensive dataset designed for evaluating tool-using agents. ToolBench is constructed upon a vast collection of real-world, high-quality REST APIs sourced from RapidAPI, a major API hub. This grounding in real-world services ensures that the tasks and tools reflect practical challenges faced by AI agents.

Overall Statistics. The full dataset encompasses 46,985 tools (APIs) organized into 129 tool collections. As mentioned in the main text, each tool is annotated with rich metadata, including a human-assigned functional category. There are 49 distinct functional categories in total (e.g., Finance, Travel, Sports, etc.), which provide a semantic grouping for the tools.

Evaluation Scenarios. ToolBench defines a standardized test set comprising 641 queries, which are categorized into three levels of increasing difficulty based on the complexity of the required tool interactions. These scenarios are:

- 810 • **Instruction 1 (I1): Single-Tool Usage.** These tasks require the agent to select and correctly
811 use a single tool to answer the user’s query. This scenario primarily tests the agent’s ability
812 for accurate tool retrieval and basic API execution.
- 813 • **Instruction 2 (I2): Intra-Category Multi-Tool Usage.** These tasks involve solving a
814 problem that requires composing a sequence of tools. Critically, all necessary tools belong
815 to the *same functional category*. This tests the agent’s ability to reason and plan within a
816 coherent semantic domain.
- 817 • **Instruction 3 (I3): Intra-Collection Multi-Tool Usage.** This is the most challenging
818 scenario. Tasks require the agent to orchestrate multiple tools that may come from *dif-
819 ferent functional categories* but are part of the same broader tool collection (e.g., a “Trip
820 Planning” collection might contain tools from “Flights”, “Hotels”, and “Maps” categories).
821 This evaluates the agent’s advanced planning and generalization capabilities across diverse
822 tool functions.

823
824 **Data Statistics for Alignment Tuning Stages.** Our training methodology is structured into two
825 main fine-tuning stages. We utilize the official splits and data provided by the ToolBench bench-
826 mark (Qin et al., 2023), processing them to fit our generative framework. The statistics for each
827 stage are detailed below:

- 828 • **Stage 1: Tool Retrieval Alignment.** The initial fine-tuning stage is designed to teach the
829 model the crucial mapping between a user’s intent and the appropriate tool. To achieve
830 this, we fine-tune the model on Query-Tool pairs extracted from ToolBench. In this super-
831 vised task, the input is a natural language query, and the target output is the corresponding
832 tool’s structured semantic code sequence. Following the data processing approach of prior
833 work (Wang et al., 2024b), we utilize a comprehensive set of 489,702 query-tool pairs,
834 aggregated across the I1, I2, and I3 scenarios, to train a robust retrieval capability.
- 835 • **Stage 2: Tool Usage Trajectory Alignment.** After the model has learned to retrieve tools,
836 the second stage trains it to function as a complete, autonomous agent. This is accom-
837 plished by fine-tuning on full execution trajectories. Each trajectory provides a complete,
838 multi-step example of how to reason, plan, generate arguments, and invoke tools to solve
839 a complex user query. We adapt the original ToolBench trajectories by replacing all tool
840 names with our learned semantic codes. For this final and most complex training step, we
841 use a total of 183,336 trajectories.

843 A.2 BASELINE DETAILS

844 In our experiments, we compare ToolWeaver against several representative retrieval and tool-use
845 models. These baselines are chosen to cover a wide range of approaches, from classic unsupervised
846 methods to state-of-the-art generative agents.

- 847 • **BM25** (Robertson & Zaragoza, 2009): An unsupervised, classical retrieval model that
848 ranks documents based on query relevance, using normalized term frequency and docu-
849 ment length. It serves as a strong lexical baseline.
- 850 • **Embedding Similarity (EmbSim):** An unsupervised semantic retrieval method. We use
851 OpenAI’s powerful text-embedding-3-large model to generate embeddings for
852 both queries and tool documents, and rank tools based on the cosine similarity of their
853 embeddings.
- 854 • **ToolRetriever** (Qin et al., 2023): A supervised, BERT-based dense retriever specifically
855 designed for tool retrieval. It is trained using contrastive learning to distinguish between
856 relevant and irrelevant tools by maximizing the similarity between queries and their corre-
857 sponding ground-truth tools.
- 858 • **ToolGen** (Wang et al., 2024b): A state-of-the-art generative model that unifies tool retrieval
859 and calling. It represents each tool as a unique atomic token and is fine-tuned to directly
860 generate the tool’s token and its arguments in response to a query.
- 861 • **ToolLlama-2** (Qin et al., 2023): A version of the Llama-2 model fine-tuned for tool use.
862 Unlike generative models like ToolGen and ToolWeaver, it relies on an external retriever to

864 first select a set of candidate tools, which are then provided in the prompt context for the
 865 model to perform reasoning and task completion.
 866

867 • **GPT-4o-mini**: A highly capable and efficient model from OpenAI. We use it as a strong
 868 baseline for end-to-end task completion. Following the StableToolBench evaluation pro-
 869 tocol (Guo et al., 2024), it also serves as the reference model for calculating the Solvable
 870 Win Rate (SoWR) metric.
 871

872 • **Re-Invoke** (Chen et al., 2024): An advanced unsupervised retrieval method that enriches
 873 tool documents by generating synthetic queries. During inference, it uses an LLM to ana-
 874 lyze user intent and employs a multi-view similarity ranking strategy to identify the most
 875 relevant tools.
 876

877 • **IterFeedback** (Xu et al., 2024): A retrieval framework that enhances a BERT-based re-
 878 triever by incorporating iterative feedback from a large language model. The LLM is
 879 prompted to analyze initial retrieval results and provide feedback to refine the search, im-
 880 proving retrieval accuracy over multiple steps.
 881

882 **A.3 IMPLEMENTATION AND TRAINING DETAILS**
 883

884 This appendix provides a detailed description of the implementation specifics for the models and
 885 experiments presented in the main paper, ensuring full reproducibility.
 886

887 The structured tokenization process begins with generating initial dense semantic embeddings for
 888 each tool. We process the textual documentation of each tool (including its name and description)
 889 using the `a11-mpnet-base-v2` model from the Sentence-Transformers library, which produces
 890 a 768-dimensional embedding. The core of our structured tokenization is a collaborative-aware
 891 residual quantization process. This process employs a multi-level scheme with $L = 2$ codebooks,
 892 \mathcal{C}_1 and \mathcal{C}_2 , each containing $K = 1024$ learnable vectors. This compositional structure represents
 893 the entire tool library with only $2 \times 1024 = 2048$ new tokens added to the LLM’s vocabulary. The
 894 initial 768-dimensional embeddings are first projected into a 64-dimensional space ($D' = 64$) using
 895 a multi-layer perceptron (MLP) with sequential hidden layer dimensions of 1024, 512, 256, and 128.
 896

897 The codebooks are trained using the AdamW optimizer with a learning rate of 1e-5 and a batch
 898 size of 5096, over 50 warmup epochs with no weight decay. For the main results, the collaborative
 899 regularization weight, λ , was set to 1.0. We initialize the codebook centroids using k-means with
 900 a maximum of 100 iterations. For conflict mitigation, the Sinkhorn-Knopp algorithm is run for 50
 901 iterations.
 902

903 The integration of these learned codes into the LLM is achieved through a two-stage generative
 904 alignment process. In Stage 1, the model is fine-tuned for 5 epochs on query-tool pairs for retrieval
 905 alignment. In Stage 2, it is fine-tuned for an additional 2 epochs on full interaction trajectories to
 906 learn complex planning. For both stages, we employ a cosine learning rate scheduler with a 3%
 907 warmup ratio and a peak learning rate of 4×10^{-5} . The input context length is truncated to 6,144
 908 tokens. All experiments were conducted on NVIDIA A100 GPUs, and we leveraged the DeepSpeed
 909 ZeRO-3 optimization suite and FlashAttention-2 to enhance training efficiency.
 910

911 **A.4 EVALUATION SETTING DETAILS**
 912

913 Our experiments adopt two distinct retrieval settings from prior work (Wang et al., 2024b): **In-**
 914 **Domain** and **Multi-Domain**. The In-Domain setting restricts the search space to a pre-filtered
 915 tool category, while the more challenging Multi-Domain setting requires the model to select from
 916 the entire global corpus of nearly 47,000 APIs for any given query. For our primary experiments
 917 presented in the main body of this paper, we focus on the Multi-Domain setting as it provides a
 918 more realistic and rigorous test of a model’s ability to handle large-scale retrieval and disambiguate
 919 tool functions. A complete set of results for both settings, including the In-Domain evaluation, is
 920 provided for reference in Appendix B.1.
 921

918
 919 Table 4: Tool retrieval evaluation across two settings: In-domain and Multi-domain. * represents the
 920 results disclosed in Wang et al. (2024b), while the others are the results we re-implemented based
 921 on the open-source checkpoints.

Model	I1			I2			I3		
	NDCG@1	NDCG@3	NDCG@5	NDCG@1	NDCG@3	NDCG@5	NDCG@1	NDCG@3	NDCG@5
In-domain									
BM25*	29.46	31.12	33.27	24.13	25.29	27.65	32.00	25.88	29.78
EmbSim*	63.67	61.03	65.37	49.11	42.27	46.56	53.00	46.40	52.73
Re-Invoke*	69.47	-	61.10	54.56	-	53.79	59.65	-	59.55
IterFeedback*	90.70	90.95	92.47	89.01	85.46	87.10	91.74	87.94	90.20
ToolRetriever*	80.50	79.55	84.39	71.18	64.81	70.35	70.00	60.44	64.70
ToolGen*	89.17	90.85	92.67	91.45	88.79	91.13	87.00	85.59	90.16
BM25	29.25	31.04	33.49	26.50	25.97	27.96	32.00	25.88	29.78
EmbSim	61.00	57.78	62.31	54.00	45.31	49.54	54.00	46.56	52.91
ToolRetriever	83.50	83.67	88.66	72.00	73.27	80.40	70.00	70.01	77.21
ToolGen	91.00	92.15	94.11	87.50	88.52	90.81	87.00	85.35	90.08
ToolWeaver	93.76	94.80	95.69	91.91	93.07	95.63	86.00	86.13	90.39
Multi-domain									
BM25*	22.77	22.64	25.61	18.29	20.74	22.18	10.00	10.08	12.33
EmbSim*	54.00	50.82	55.86	40.84	36.67	39.55	18.00	17.77	20.70
ToolRetriever*	72.31	70.30	74.99	64.54	57.91	63.61	52.00	39.89	42.92
ToolGen*	87.67	88.84	91.54	83.46	86.24	88.84	79.00	79.80	84.79
BM25	26.92	26.13	29.00	20.00	21.92	23.46	10.00	10.08	12.33
EmbSim	50.50	48.15	53.41	46.00	39.58	43.05	18.00	17.77	20.94
ToolRetriever	75.92	76.96	82.31	63.00	66.38	72.72	28.00	39.28	44.54
ToolGen	88.50	88.83	91.65	84.00	85.65	89.02	81.00	80.83	85.83
ToolWeaver	91.16	91.14	93.48	89.76	89.70	91.80	88.00	85.80	90.12

B SUPPLEMENTARY EXPERIMENTAL RESULTS

B.1 EXTENDED RESULTS ON MAIN EXPERIMENTS

This section provides a more detailed and comprehensive view of our experimental results, supplementing the key findings presented in the main paper. While the main text focused on the most challenging Multi-Domain setting to rigorously evaluate ToolWeaver’s performance in a realistic, large-scale environment, we present results for both In-Domain and Multi-Domain settings here for completeness and to facilitate a thorough comparison with prior work.

Tables 4 and 5 offer a complete breakdown of the tool retrieval evaluation. We include results reported by the original authors of baseline methods (*) alongside our own reproductions. The strong alignment between our re-implemented results and those originally published for models like ToolGen validates the fairness and correctness of our experimental setup. Even in the In-Domain setting, where the search space is constrained, ToolWeaver demonstrates top-tier performance. It is particularly noteworthy that ToolWeaver, as a single end-to-end model, outperforms complex, multi-stage retrieval systems like IterFeedback in most scenarios, highlighting the efficiency of our generative approach. Furthermore, Table 5 provides the full generalization results, reinforcing the findings from the main paper that ToolWeaver’s learned collaborative semantics transfer effectively to unseen tools and categories.

In Table 6, we expand on the end-to-end task completion evaluation. For full transparency, this table includes results from prior work (*) alongside our own. It is important to note potential differences in evaluation protocols. For example, some prior results were obtained using GPT-3.5 as the core agent and evaluator. Considering that GPT-3.5 is no longer a state-of-the-art model and its usage can be costly, we chose to standardize our evaluation using the more recent and capable GPT-4o-mini as both a strong baseline and, for SoWR, the reference judge. This ensures a consistent and modern benchmark for all models we tested. Despite these variations, ToolWeaver consistently demonstrates superior or highly competitive performance. Its significant lead in complex multi-step tasks (I3) and generalization scenarios remains evident, underscoring the benefits of its collaborative-aware tokenization for robust task planning and execution. We also include the SoWR results for GPT-4o-mini in this table for completeness; however, similar to observations in other studies, we noted a tendency for the model to favor its own solutions, which is why we focused on comparing the fine-tuned models in the main text to ensure a fair assessment.

972
973
974
Table 5: Tool retrieval evaluation under In-domain and Multi-domain settings, including results on
975 **I1-Tool.**, **I1-Cat.**, and **I2-Cat.** subsets.
976

Model	I1-Tool.			I1-Cat.			I2-Cat.		
	NDCG@1	NDCG@3	NDCG@5	NDCG@1	NDCG@3	NDCG@5	NDCG@1	NDCG@3	NDCG@5
In-domain									
BM25	28.00	31.37	33.06	31.12	30.87	33.13	21.75	24.75	27.44
EmbSim	61.50	58.74	62.99	69.00	66.43	71.00	44.22	39.18	43.50
ToolRetriever	79.50	81.54	86.78	80.50	81.68	87.15	70.35	74.09	81.45
ToolGen	89.50	91.61	93.34	87.50	88.79	91.21	88.44	88.85	91.34
ToolWeaver	92.00	92.91	93.87	91.00	91.92	92.93	92.46	92.27	92.82
Multi-domain									
BM25	20.75	21.12	23.64	20.63	20.67	24.18	16.58	19.55	20.89
EmbSim	53.00	49.82	54.93	58.00	54.38	59.24	35.68	33.92	36.22
ToolRetriever	75.25	78.26	83.08	73.50	73.56	79.10	60.30	64.11	73.01
ToolGen	84.00	86.40	89.52	89.50	89.95	92.01	83.42	86.06	88.47
ToolWeaver	86.50	88.44	90.72	92.50	90.75	92.30	89.45	88.19	89.85

985
986
987
Table 6: Tool calling evaluation performance on unseen instructions and unseen tools under two
988 settings. Bold values denote the highest performance, considering only the results reproduced in our
989 experimental setting.
990

Model	Setting	SoPR						SoWR					
		I1	I2	I3	I1-Tool.	I1-Cat.	I2-Cat.	I1	I2	I3	I1-Tool.	I1-Cat.	I2-Cat.
GPT-3.5*	Retrieval	51.43	41.19	34.43	57.59	53.05	46.51	53.37	53.77	37.70	46.20	54.25	54.81
ToolLlama-2*	Retrieval	56.13	49.21	34.70	-	-	-	50.92	53.77	21.31	-	-	-
ToolLlama*	Retrieval	54.60	49.96	51.37	57.70	61.76	45.43	49.08	61.32	31.15	48.73	50.98	44.35
ToolGen*	Retrieval	56.13	52.20	47.54	56.54	49.46	51.96	50.92	62.26	34.42	40.51	39.87	37.90
GPT-4o-mini	Retrieval	52.25	40.41	24.86	53.16	50.11	39.38	47.24	52.83	44.26	49.37	50.33	42.74
ToolLlama-2	Retrieval	28.94	24.69	10.93	28.48	36.93	19.09	25.15	30.19	24.59	26.58	27.45	20.16
ToolGen		52.97	45.13	36.34	45.36	55.56	45.56	36.20	42.45	49.18	32.91	42.48	37.90
ToolWeaver		53.17	44.03	52.19	54.85	57.41	46.24	40.49	48.11	59.02	36.08	43.14	35.48

991
992
993
994
995
996
997
998
B.2 DETAILED COMPARISON OF TOKENIZATION STRATEGIES
9991000
1001
1002
1003
To provide a comprehensive evaluation of our tokenization strategy, we implemented and compared
1004 it against several representative baseline methods. This section describes these alternatives. For all
1005 methods, we follow the same two-stage generative alignment tuning process described in Section 3.3
1006 to ensure a fair comparison of the representation strategies themselves.
10071008
1009
1010
The detailed performance results for tool retrieval and end-to-end task completion are presented in
1011 Table 7 and Table 8, respectively. These tables provide the underlying data for the summary chart in
1012 Figure 4 of the main paper.
10131014
1015
1016
1017
Table 7: Retrieval performance (NDCG@k) of different tokenization methods. ToolWeaver’s ap-
1018 proach of integrating collaborative semantics into a structured representation yields the best perfor-
1019 mance, especially in complex multi-tool scenarios (I2, I3).
1020

Tokenization	NDCG@1			NDCG@3			NDCG@5		
	I1	I2	I3	I1	I2	I3	I1	I2	I3
Numerical	81.55	76.93	71.88	83.61	77.02	75.94	85.13	78.29	79.45
Hierarchical	86.72	77.50	78.21	85.93	78.82	80.56	89.14	83.11	86.73
Semantic	89.13	83.88	83.15	90.82	84.01	78.84	92.15	87.93	86.99
Atomic	87.67	83.46	79.00	88.84	86.24	79.80	91.54	88.84	84.79
ToolWeaver	91.16	89.76	88.00	91.14	89.70	85.80	93.48	91.80	90.12

1021
1022
1023
1024
1025
Atomic Tokenization. This is a widely-used baseline in generative tool-use models (Wang et al.,
2024b). Each tool is represented by a single, unique special token. Specifically, the API function
“compress” from the RESTful API “IMAGON” is tokenized into a single composite token like
<<IMAGON&&compress>>. These new tokens are added to the LLM’s vocabulary. While simple,
this approach suffers from a linear growth in vocabulary size and fails to capture any semantic or
collaborative relationships between tools, as their representations are learned independently. The
results for this baseline are adopted from our ToolGen implementation.
1026

1026 Table 8: End-to-end task completion performance (SoPR/SoWR) for different tokenization methods.
 1027 All methods shown generate tool tokens directly, without the need for a retriever. The superior
 1028 retrieval accuracy of ToolWeaver translates directly into higher task success rates.

Tokenization	SoPR					SoWR						
	I1	I2	I3	I1Tool.	I1Cat.	I2Cat.	I1	I2	I3	I1Tool.	I1Cat.	I2Cat.
Numerical	21.98	9.12	11.20	20.68	26.14	17.20	16.56	16.04	16.39	20.89	23.53	14.52
Hierarchical	39.16	20.28	17.49	36.29	31.81	14.92	29.45	28.30	26.23	29.11	24.83	14.52
Semantic	50.20	28.91	16.39	33.02	51.42	27.02	39.26	29.24	32.79	29.11	43.79	22.58
Atomic	52.97	45.13	36.34	45.36	55.56	45.56	36.20	42.45	49.18	32.91	42.48	37.90
ToolWeaver	53.17	44.03	52.19	54.85	57.41	46.24	40.49	48.11	59.02	36.08	43.14	35.48

1036
 1037 **Numerical Tokenization.** This serves as a simple, non-semantic baseline. Each tool is mapped
 1038 to a unique numeric string of fixed length. For a library of 47,000 tools, a five-digit string is used.
 1039 For example, the 3rd tool in the corpus is represented as 0 0 0 0 3. This method creates a very
 1040 small vocabulary overhead (only 10 digit tokens) but provides no semantic or structural priors to the
 1041 model, forcing it to learn tool meanings from scratch.

1042
 1043 **Hierarchical Tokenization.** This method adopts the hierarchical coding scheme from prior work
 1044 (Wang et al., 2024b). Each tool is represented by a path in a pre-defined hierarchical structure,
 1045 resulting in a sequence of numerical codes (e.g., 1 0 1 4 0). This approach provides a structural prior
 1046 by grouping related tools. However, since the hierarchy is based on static features, it may not fully
 1047 capture the dynamic, collaborative relationships required for complex downstream tasks.

1048
 1049 **Semantic Tokenization.** This approach uses human-readable, semantically meaningful parts of
 1050 the tool’s name or function as its representation. Instead of creating abstract IDs, it directly tokenizes
 1051 the API’s function name. For instance, an API function named `compress_for_imagon` would
 1052 be represented by the sequence of its natural language tokens. This method leverages the LLM’s
 1053 existing linguistic knowledge but may struggle with APIs that have non-descriptive or ambiguous
 1054 names. It also does not explicitly model the relationships between different tools.

B.3 FULL RESULTS ON QWEN MODELS

1055
 1056 To demonstrate the generalizability and robustness of the ToolWeaver framework beyond a single
 1057 model architecture, we conducted supplementary experiments using the Qwen-2.5 model family,
 1058 with the 1.5B, 3B, 7B and 14B parameter versions. We replicated our tool retrieval evaluation,
 1059 comparing ToolWeaver directly against the strong generative baseline, ToolGen, which employs the
 1060 “one-token-per-tool” paradigm.

1061
 1062 The comprehensive results are presented in Table 9. The findings consistently show that ToolWeaver
 1063 outperforms ToolGen across all tested model sizes and evaluation settings. Notably, the performance
 1064 advantage of ToolWeaver is most pronounced in the more complex, multi-tool scenarios (I2 and I3),
 1065 reinforcing our core claim that the collaborative-aware tokenization is crucial for sophisticated rea-
 1066 soning. This trend holds across different model scales. While the performance gap narrows slightly
 1067 as model size increases, ToolWeaver maintains a consistent edge, highlighting the fundamental ef-
 1068 ficiency of its structured, collaborative-aware tokenization. The advantage is particularly significant
 1069 for the smaller 1.5B model, suggesting that our approach provides a crucial structural prior that is
 1070 especially beneficial for models with lower capacity.

1071
 1072 Furthermore, the superior performance on the generalization splits (I1-Tool, I1-Cat, and I2-Cat)
 1073 reinforces that the learned semantic structure is robust and transfers effectively to unseen tools and
 1074 categories, regardless of the underlying LLM architecture. Overall, these findings validate that the
 1075 benefits of ToolWeaver are not confined to a specific base model but represent a more general and
 1076 robust improvement for enabling scalable tool use in large language models.

B.4 EXTENDED ANALYSIS ON GENERAL LANGUAGE CAPABILITIES

1077
 1078 To investigate the impact of large-scale vocabulary expansion on an LLM’s foundational abilities,
 1079 we evaluated model performance on a suite of general NLP benchmarks. Integrating a vast toolset of

1080
1081
1082
1083
1084
1085
1086
1087
1088
1089
1090
1091

Table 9: Tool retrieval evaluation performance comparison between ToolGen and ToolWeaver across different Qwen-2.5 model sizes. For each model size, performance is measured by NDCG@k across query complexities (I1-I3) and generalization settings (I1-Tool, I1-Cat, I2-Cat).

Method	NDCG@1			NDCG@3			NDCG@5		
	I1	I2	I3	I1	I2	I3	I1	I2	I3
Qwen-2.5-1.5B									
ToolGen	88.00	84.96	69.00	89.55	84.40	71.15	91.98	88.15	80.82
ToolWeaver	89.67	88.22	87.00	89.99	87.73	87.58	91.71	89.34	89.90
	I1-Tool	I1-Cat	I2-Cat	I1-Tool	I1-Cat	I2-Cat	I1-Tool	I1-Cat	I2-Cat
ToolGen	86.00	87.00	86.93	87.79	89.28	85.14	90.81	91.21	88.70
ToolWeaver	88.50	92.00	88.44	88.59	92.25	88.18	90.93	92.83	89.92
Qwen-2.5-3B									
ToolGen	90.33	85.21	85.00	90.32	84.29	81.10	93.04	88.58	87.76
ToolWeaver	90.67	88.47	88.00	91.66	89.08	87.63	92.99	90.28	90.95
	I1-Tool	I1-Cat	I2-Cat	I1-Tool	I1-Cat	I2-Cat	I1-Tool	I1-Cat	I2-Cat
ToolGen	88.50	89.00	86.43	89.60	89.76	85.73	91.77	92.51	89.34
ToolWeaver	90.50	91.00	90.95	91.91	92.23	90.61	93.29	92.76	91.77
Qwen-2.5-7B									
ToolGen	91.83	89.22	80.00	92.31	88.22	82.98	94.38	91.74	86.58
ToolWeaver	92.50	91.23	85.00	92.89	90.49	88.52	93.98	91.89	90.73
	I1-Tool	I1-Cat	I2-Cat	I1-Tool	I1-Cat	I2-Cat	I1-Tool	I1-Cat	I2-Cat
ToolGen	91.00	92.50	89.95	91.09	92.79	88.91	93.02	94.99	92.13
ToolWeaver	91.00	94.00	90.95	92.32	94.05	90.38	93.95	94.27	91.41
Qwen-2.5-14B									
ToolGen	90.66	89.22	82.00	91.55	88.56	81.79	93.84	91.36	88.28
ToolWeaver	91.00	91.23	85.00	91.97	90.34	83.16	93.22	91.97	88.46
	I1-Tool	I1-Cat	I2-Cat	I1-Tool	I1-Cat	I2-Cat	I1-Tool	I1-Cat	I2-Cat
ToolGen	88.5	90.5	89.94	90.09	91.60	89.11	92.48	93.81	91.60
ToolWeaver	90.00	93.00	92.96	92.18	92.68	91.13	93.75	93.51	92.36

1126
1127
1128
1129
1130
1131
1132
1133

1134 nearly 47,000 APIs presents a critical trade-off between task-specific specialization and the preser-
 1135 vation of an LLM’s general language capabilities. We assessed this impact across three dimensions:
 1136 general understanding, language modeling distribution, and text generation quality.
 1137

1138 B.4.1 EVALUATION SETUP

1139 All evaluations were conducted using the open-source Language Model Evaluation Harness (Gao
 1140 et al., 2024a), version 0.4.3, ensuring standardized prompting and scoring. For **Language Mod-
 1141 eling**, we employed a sliding window approach with a window size and stride of 2,048 tokens
 1142 (non-overlapping) using the base model’s tokenizer. For **Text Summarization**, to ensure efficiency,
 1143 we evaluated a random subset of 500 samples for each task. We report ROUGE scores for n-gram
 1144 overlap and BERTScore (F1) using “roberta-large” for semantic similarity.
 1145

1146 B.4.2 BENCHMARK DESCRIPTIONS

1147 We used a diverse set of benchmarks to evaluate the models:

- 1149 • **MMLU** (Massive Multitask Language Understanding) (Hendrycks et al., 2021): A com-
 1150 prehensive benchmark covering 57 subjects to test world knowledge and problem-solving
 1151 ability.
- 1152 • **BoolQ** (Boolean Questions) (Clark et al., 2019): A reading comprehension dataset consist-
 1153 ing of yes/no questions.
- 1154 • **PIQA** (Physical Interaction Question Answering) (Bisk et al., 2020): A commonsense
 1155 reasoning benchmark testing understanding of everyday physical situations.
- 1156 • **HellaSwag** (Zellers et al., 2019): A commonsense inference task that challenges models to
 1157 choose the most plausible completion for a given text context.
- 1158 • **OpenBookQA** (Mihaylov et al., 2018): A science question-answering dataset requiring
 1159 reasoning with a small set of common knowledge facts. For this benchmark, we report
 1160 normalized accuracy.
- 1161 • **WinoGrande** (Sakaguchi et al., 2020): A commonsense reasoning dataset focused on pro-
 1162 noun resolution, designed to be robust against statistical biases.
- 1163 • **WikiText-2** (Merity et al., 2016): A standard language modeling benchmark. We use the
 1164 validation split to measure Perplexity (PPL) and Negative Log-Likelihood (NLL).
- 1165 • **CNN/DailyMail** (See et al., 2017): An abstractive summarization dataset consisting of
 1166 news articles.
- 1167 • **XSum** (Narayan et al., 2018): A dataset requiring highly abstractive, single-sentence sum-
 1168 maries from BBC articles.

1171 B.4.3 FULL EXPERIMENTAL RESULTS

1172 **General Understanding Benchmarks.** The results for tasks such as MMLU, BoolQ, and PIQA
 1173 are presented in Table 10. The data shows that the “one-token-per-tool” approach, embodied by
 1174 ToolGen, comes at a catastrophic cost to the model’s core competencies. Its average performance
 1175 plummets by nearly 23 points (from 66.81% to 43.87%) compared to the original Llama-3-8B
 1176 model. In stark contrast, ToolWeaver demonstrates far more effective management of this trade-
 1177 off. While specialization still incurs a cost, our logarithmically scaled vocabulary results in a much
 1178 more contained degradation of only 8.4 points. Crucially, this means ToolWeaver mitigates over
 1179 63% of the performance loss seen with the naive generative approach.

1180 Table 10: Performance on general NLP benchmarks. Scores are accuracy (%). For OpenBookQA,
 1181 the score represents normalized accuracy.

1183 Model	MMLU	BoolQ	PIQA	HellaSwag	OpenBookQA*	WinoGrande	Avg.
1184 Llama-3-8B (Base)	62.19	81.10	79.43	60.07	45.00	73.09	66.81
1185 ToolGen	23.52	62.17	60.07	31.60	31.00	54.85	43.87
1186 ToolWeaver	41.93	78.20	74.54	51.19	38.40	65.98	58.37

1188
 1189 **Language Modeling Distribution.** To evaluate the integrity of the model’s probability distribution,
 1190 we report the perplexity on WikiText-2 in Table 11. ToolGen exhibits a severe explosion in
 1191 perplexity, reaching 104.54, which indicates a significant disruption to the natural language distribution
 1192 likely caused by the massive injection of initialized tokens. Conversely, ToolWeaver maintains
 1193 a much lower perplexity of 25.36. This result suggests that our structured, collaborative-aware codes
 1194 integrate more harmoniously with the pre-trained weights, preserving the model’s ability to predict
 1195 natural language sequences.

1196 Table 11: Language modeling evaluation on WikiText-2 (Validation Split).

Model	Avg NLL	Perplexity
Llama-3-8B (Base)	1.847	6.34
ToolWeaver	3.233	25.36
ToolGen	4.650	104.54

1204 **Text Generation Quality.** We assessed generation capabilities via zero-shot summarization, as
 1205 detailed in Table 12. On the CNN/DailyMail dataset, ToolWeaver performs nearly on par with the
 1206 Base LLM (BERTScore 0.8507 vs. 0.8535). On the more challenging XSum dataset, which requires
 1207 high-level abstraction, ToolGen suffers a notable drop in precision (ROUGE-2 drops to 0.0175). In
 1208 comparison, ToolWeaver retains robust generation capabilities (ROUGE-2 0.0261). These results
 1209 confirm that ToolWeaver not only preserves understanding but also maintains the ability to generate
 1210 coherent and accurate text, a capability that is often compromised in standard generative tool
 1211 learning methods.

1212 Table 12: Zero-shot summarization performance (Means over 500 samples).

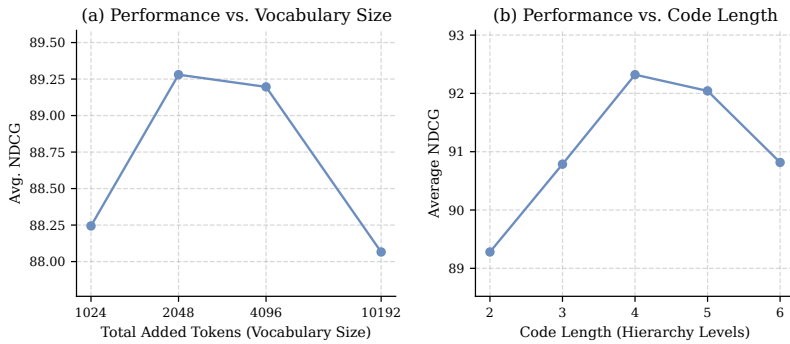
Model	CNN/DailyMail				XSum			
	BERTScore	R-1	R-2	R-L	BERTScore	R-1	R-2	R-L
Llama-3-8B (Base)	0.8535	0.2107	0.0856	0.1501	0.8505	0.1494	0.0376	0.1060
ToolGen	0.8293	0.1541	0.0535	0.1127	0.8253	0.0969	0.0175	0.0702
ToolWeaver	0.8507	0.2021	0.0813	0.1461	0.8418	0.1240	0.0261	0.0872

1221 **B.5 CODEBOOK HYPERPARAMETER SENSITIVITY ANALYSIS**

1222 To empirically validate the design choices of ToolWeaver, we conduct a sensitivity analysis on two
 1223 critical hyperparameters governing the structured tokenization: the total size of the added vocabulary
 1224 and the depth of the hierarchical code (code length).

1228 **Impact of Vocabulary Size.** We first investigate how the total number of added tokens affects
 1229 retrieval performance. In this experiment, we maintain a fixed code length of $L = 2$ while varying
 1230 the size K of the codebooks at each layer. We specifically evaluated configurations with equal
 1231 layer sizes of $K \in \{512, 1024, 2048, 5096\}$, which correspond to total added vocabulary sizes of
 1232 1,024, 2,048, 4,096, and 10,192 tokens, respectively. As illustrated in Figure 5(a), the Average
 1233 NDCG exhibits an inverted U-shape, peaking at the 1024×2 configuration (2,048 tokens). When
 1234 the codebook is too small (512×2), performance is suboptimal, likely due to code collision where
 1235 functionally distinct tools are forced to map to the same identifiers. Crucially, as we increase the size
 1236 to 2048×2 and further to 5096×2 (totaling 10,192 tokens), we observe a significant performance
 1237 drop. This decline confirms our hypothesis regarding the sparsity of collaborative signals: as the
 1238 vocabulary grows towards the “one-token-per-tool” extreme, the probability of related tools sharing
 1239 a common code decreases. This dilutes the dense co-occurrence patterns ToolWeaver relies on.
 1240 Consequently, our default setting of 1024×2 strikes the optimal balance between representational
 1241 capacity and signal density.

1242
 1243 **Impact of Code Length.** Next, we evaluate the effect of the code sequence length L , which cor-
 1244 responds to the depth of the quantization hierarchy. We fix the codebook size per layer at $K = 1024$
 1245 and vary L from 2 to 6. Figure 5(b) shows that performance improves significantly as the hierarchy
 1246 deepens, reaching a peak at $L = 4$. This trend suggests that a deeper hierarchy captures finer-grained
 1247 semantic nuances, aiding in precise tool disambiguation. However, performance begins to degrade
 1248 as the length extends beyond 4 layers, dropping to 90.82 at $L = 6$. We attribute this degradation
 1249 primarily to the increased difficulty of autoregressive generation, where longer sequences heighten
 1250 the risk of error propagation during decoding, and potentially to the diminishing returns of residual
 1251 quantization at deeper layers. Although $L = 4$ offers the highest theoretical performance, we utilize
 1252 $L = 2$ in our main experiments to maintain a favorable trade-off between retrieval accuracy and
 1253 inference efficiency.



1254
 1255 **Figure 5: Hyperparameter sensitivity analysis. (a) Performance vs. Vocabulary Size:** Evaluated
 1256 with fixed code length $L = 2$. Performance peaks at 2,048 tokens, confirming that a compact
 1257 vocabulary fosters better collaborative learning than a sparse, large one. **(b) Performance vs. Code**
 1258 **Length:** Evaluated with fixed codebook size $K = 1024$. While deeper hierarchies ($L = 4$) improve
 1259 semantic resolution, excessively long sequences ($L = 6$) degrade performance due to generation
 1260 complexity.

B.6 SINKHORN-KNOPP EFFICIENCY AND STABILITY ANALYSIS

1261 To ensure that the conflict mitigation mechanism via uniform mapping does not introduce computa-
 1262 tional bottlenecks or numerical instability, we conducted a comprehensive profiling analysis of the
 1263 Sinkhorn-Knopp algorithm during the training of ToolWeaver.

B.6.1 EXPERIMENTAL SETUP

1264 We profiled the training process on a single NVIDIA A100-SXM4-80GB GPU, using the full Tool-
 1265 Bench embedding matrix ($46,984 \times 768$) and a batch size of $B = 5,096$, consistent with our main
 1266 experiments described in Appendix A.3. The model employs two codebooks ($L = 2$) with 1,024
 1267 codes each. In this configuration, the Sinkhorn-Knopp algorithm is invoked exactly twice per opti-
 1268 mizer step (once for each codebook’s assignment) to enforce uniformity constraints. To analyze the
 1269 trade-off between stability and cost, we fixed the number of Sinkhorn iterations at 50 and swept the
 1270 entropy regularization parameter ϵ across values of $\{0.005, 0.01, 0.02\}$.

B.6.2 RESULTS AND DISCUSSION

1271 **Computational Cost Analysis.** We analyzed the steady-state training time per step after the initial
 1272 warm-up phase. The average total time per training step is 0.161 seconds. Of this, the two Sinkhorn
 1273 solves consume a combined average of 0.0283 ± 0.0002 seconds (approximately 14.15 ms per call).
 1274 This corresponds to a computational overhead of only **17.6%** of the total step time. The vast majority
 1275 of the computation ($\sim 82\%$) is dedicated to the encoder/decoder MLP layers and the backward pass.
 1276 These results empirically verify that the Sinkhorn integration is computationally efficient and does
 1277 not constitute a bottleneck for training scalability.

Figure 6: A real RESTful API example for extracting information from a Thai driver's license, including details like the API's endpoint, parameters, and code snippet for implementation.

Stability and Uniformity. Numerical stability is critical for optimal transport algorithms. Throughout our profiling of 20 consecutive batches, we observed no NaN or Inf values, confirming the numerical robustness of our implementation. Regarding uniformity, with our chosen setting of $\epsilon = 0.01$, the final residual assignments remain highly balanced. The standard deviation of tool counts per code is 1.38 (against a theoretical target of 4.97 tools per code), with 95% of codes receiving between 3 and 7 assignments per batch. This indicates that the algorithm successfully mitigates index collapse without enforcing an overly rigid permutation.

Ablation on Entropy Regularization (ϵ). We further analyzed the impact of ϵ on performance. As summarized in Table 13, $\epsilon = 0.01$ provides the optimal balance. Strict regularization ($\epsilon = 0.005$) sharpens the distribution (Rel. Std 0.19) but increases overhead to 20.3% due to slower convergence. Conversely, loose regularization ($\epsilon = 0.02$) degrades uniformity (Rel. Std 0.47) without improving runtime. This justifies our choice of $\epsilon = 0.01$ for the main experiments.

Table 13: Profiling results for Sinkhorn-Knopp at varying entropy regularization levels (ϵ). The chosen setting ($\epsilon = 0.01$) provides the best trade-off between runtime overhead and uniformity.

ϵ Setting	Step Overhead (%)	Time per Call (ms)	Uniformity (Rel. Std)	Conclusion
0.005 (Strict)	20.3%	18.9	0.19	Slower convergence
0.01 (Ours)	17.6%	14.2	0.28	Optimal balance
0.02 (Loose)	17.5%	14.1	0.47	Degraded uniformity

B.7 INFERENCE LATENCY AND MEMORY ANALYSIS

While ToolWeaver achieves logarithmic scalability regarding vocabulary size, representing a single tool as a sequence of L codes naturally introduces more decoding steps compared to the atomic “one-token-per-tool” approach used in baselines like ToolGen. To rigorously assess the practical cost of this design, we conducted a systematic evaluation of decoding latency, throughput, and memory consumption.

```

1350
1351
1352
1353
1354
1355
1356
1357
1358
1359
1360
1361
1362
1363
1364
1365
1366
1367
1368
1369
1370
1371
1372
1373
1374
1375
1376
1377
1378
1379
1380
1381
1382
1383
1384
1385
1386
1387
1388
1389
1390
1391
1392
1393
1394
1395
1396
1397
1398
1399
1400
1401
1402
1403
{
  "tool_name": "URL to QRCode Image API",
  "tool_description": "This API takes URL and return as a QR Code image",
  "title": "URL to QRCode Image API",
  "pricing": "FREEUMIUM",
  "score": null,
  "home_url": "https://rapidapi.com/ohidur/api/url-to-qrcode-image-api/",
  "host": "url-to-qrcode-image-api.p.rapidapi.com",
  "api_list": [
    {
      "name": "QR Code Image",
      "url": "https://url-to-qrcode-image-api.p.rapidapi.com/qr",
      "description": "This endpoint takes a 'GET' request with url or string as a parameter and returns QR code image",
      "method": "GET",
      "required_parameters": [],
      "optional_parameters": [
        {
          "name": "url",
          "type": "STRING",
          "description": "",
          "default": "https://www.google.com"
        }
      ],
      "code": "import requests\nurl = \"https://url-to-qrcode-image-api.p.rapidapi.com/qr\"\nquerystring = {\n    \"url\": url\n}\nheaders = {\n    \"X-RapidAPI-Key\": \"SIGN-UP-FOR-KEY\"\n}\nX-RapidAPI-Host: \"url-to-qrcode-image-api.p.rapidapi.com\"\nresponse = requests.get(url, headers=headers,\n    params=querystring)\nprint(response.json())\n",
      "statuscode": 200,
      "body": "",
      "headers": "",
      "schema": ""
    }
  ]
}

```

Figure 7: A real tool example. It shows the details of the “URL to QRCode Image API”, including its description, endpoint, method, parameters, and a code snippet for implementation.

B.7.1 EXPERIMENTAL SETUP

We measured the inference performance on a single NVIDIA A100-80GB GPU. To ensure a fair comparison, we evaluated both ToolGen (Atomic) and ToolWeaver with varying codebook depths ($L \in \{2, 3, 4\}$) and a fixed codebook size of $K = 1024$. The metrics were averaged across the I1, I2, and I3 retrieval tasks to cover varying query complexities. We report:

- **Avg Latency (ms):** The average wall-clock time required to decode the tool identifier(s) for a single query.
- **P95 Latency (ms):** The 95th percentile latency, reflecting worst-case performance.
- **Avg Throughput (Tok/s):** The number of tokens generated per second during the decoding phase.
- **Peak GPU Memory (GB):** The maximum GPU memory allocated during inference.

B.7.2 RESULTS AND DISCUSSION

The results are summarized in Table 14. We observe the following trends:

Table 14: Inference efficiency comparison. We compare the atomic baseline (ToolGen) against ToolWeaver with increasing codebook depths (L). While latency increases linearly with depth due to longer sequence generation, the absolute overhead is minimal ($\sim 20\text{-}75\text{ms}$). Crucially, ToolWeaver maintains a lower and constant memory footprint.

Model Configuration	Representation Structure	Avg Latency (ms)	P95 Latency (ms)	Throughput (Tok/s)	Peak Memory (GB)
ToolGen (Baseline)	Atomic (1-level)	108.16	111.98	19.54	15.77
ToolWeaver ($L = 2$)	[1024, 1024]	128.21	132.43	24.53	15.08
ToolWeaver ($L = 3$)	[1024, 1024, 1024]	157.65	165.73	26.34	15.10
ToolWeaver ($L = 4$)	[1024, 1024, 1024, 1024]	183.14	189.11	28.26	15.11

Latency Trade-off is Acceptable. As expected, latency increases linearly with the number of codebook layers. Comparing the standard $L = 2$ setting of ToolWeaver to ToolGen, the overhead

per query is approximately 20ms (108.16ms vs. 128.21ms). Even with a deeper hierarchy ($L = 4$), the total latency remains under 200ms. In the context of tool-augmented agents, where executing an external API call typically consumes hundreds of milliseconds to seconds, this decoding overhead is negligible. This confirms that the trie-constrained decoding over a hierarchical code space is highly efficient for online deployment.

Higher Token Throughput. Interestingly, ToolWeaver exhibits higher token throughput (Tok/s) as L increases. This is a natural consequence of the hierarchical representation: decoding a single logical tool requires generating L simpler code tokens. Since the computational cost per step is dominated by the transformer’s forward pass (which remains constant), generating a sequence of cached code-tokens allows the system to amortize the overhead, resulting in higher apparent throughput (19.54 vs. 28.26 Tok/s). This indicates that the model’s generation speed is not bottlenecked by the codebook lookup.

Memory Efficiency. A significant advantage of ToolWeaver is its memory efficiency. ToolGen requires maintaining a massive embedding table and LM head for nearly 47,000 atomic tool tokens, resulting in a peak memory usage of ~ 15.77 GB. In contrast, ToolWeaver reduces the vocabulary expansion to a logarithmic scale (e.g., 2×1024 tokens), keeping the peak memory stable at ~ 15.10 GB across all settings. This saving of approximately 0.67 GB is substantial for deploying LLMs on memory-constrained edge devices, validating our claim that ToolWeaver is a more scalable solution for massive tool libraries.

B.8 FAILURE ANALYSIS

To investigate the limitations of ToolWeaver, we analyzed error cases in the end-to-end evaluation. We categorize the **first occurring error** in a trajectory using a strict hierarchical logic: First, we check Process Consistency; if the predicted step index exceeds or falls short of the ground truth length, it is labeled as **Redundant** or **Incomplete Process**, respectively. Second, if the length is valid but the predicted identifier mismatches the ground truth, it is marked as **Wrong Tool**. Finally, if the tool is correct but fails due to parsing errors, missing fields, or runtime exceptions, it is categorized as **Wrong Parameters**. Figure 8 illustrates the distribution of these errors.

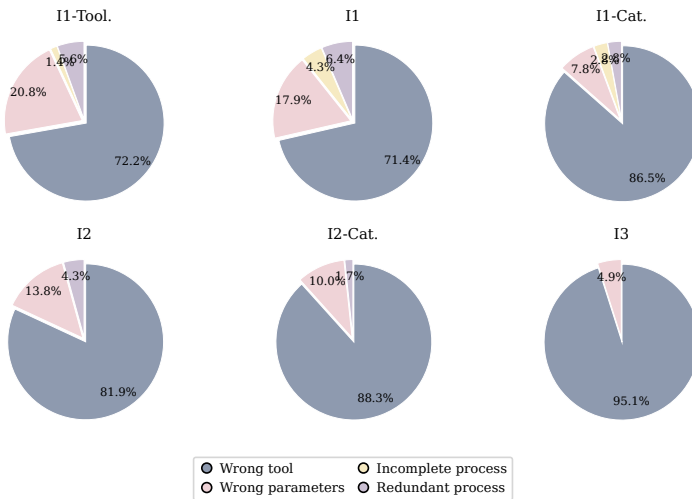


Figure 8: Distribution of failure types across ToolBench scenarios (I1-I3) and generalization splits (Tool/Cat).

The distribution reveals a clear shift in failure modes across different stages of complexity. Wrong Tool (Blue) is the dominant error, increasing significantly from I1 (71%) to I3 (95%). This indicates that as the reasoning chain grows longer and more complex (I3), the primary bottleneck becomes the precise retrieval of the correct API from the massive 47k corpus, rather than planning length. Consequently, Wrong Parameters (Pink) shows a stable presence (10–20%) in simpler scenarios

1458 (I1/I2), suggesting that once the model successfully locates the correct tool, its ability to comprehend
 1459 API schemas and generate valid arguments is relatively robust. However, in I3, the parameter error
 1460 rate drops artificially (4.9%) simply because the model rarely passes the initial tool selection check.
 1461 Similarly, Incomplete/Redundant processes are visible in simpler tasks but vanish in complex ones,
 1462 confirming that in multi-step scenarios, the agent struggles primarily with semantic discrimination
 1463 of tools before it can even exhibit planning or formatting faults.

1464 C QUALITATIVE ANALYSIS AND EXAMPLES

1465 C.1 CASE STUDY: ANALYSIS OF LEARNED TOOL CODES AND MULTI-TOOL 1466 COORDINATION

1470 This section provides a detailed qualitative analysis of the hierarchical codes learned by ToolWeaver.
 1471 By examining the tool clusters formed under specific high-level codes, we interpret their emergent
 1472 semantic meaning. Furthermore, we analyze a real execution trajectory to illustrate how these shared
 1473 parent codes facilitate complex multi-tool coordination.

1474 C.1.1 DETAILED ANALYSIS OF LEARNED STRUCTURES

1475 We observe that the model learns meaningful abstractions ranging from service encapsulation to
 1476 functional decomposition. Below we detail three specific cases:

1477 **Case 1: Clear Service Encapsulation (<T1_747>).** This high-level code has learned to cleanly
 1478 encapsulate tools related to the video game “Guild Wars 2”. An analysis of the 97 tools sharing
 1479 this primary code confirms this, showing a perfect 100% alignment with the ground-truth *Gaming*
 1480 category. Representative tools include:

- 1481 • Get Account Info (from the “Guild Wars 2” service)
- 1482 • Get Achievements (from the “Guild Wars 2” service)
- 1483 • Get Character Hero Points (from the “Guild Wars 2” service)
- 1484 • Get Pvp Stats (from the “Guild Wars 2” service)

1485 While this grouping alone demonstrates strong semantic clustering, its true value lies in creating the
 1486 prerequisite for learning collaboration. By sharing the parent code <T1_747>, these tools provide
 1487 a dense, shared signal during training. This allows the model to efficiently learn that these tools are
 1488 often co-utilized to answer complex queries about the game, overcoming the signal sparsity issue
 1489 inherent in methods that use monolithic, independent tool IDs.

1490 **Case 2: Hierarchical Functional Decomposition (<T1_184>).** This case highlights the model’s
 1491 ability to perform functional decomposition, grouping tools related to Billboard music charts. All
 1492 92 tools under this code correctly belong to the *Music* category. The model correctly groups tools
 1493 like Hot 100 (from the “Billboard” service) and New Zealand Songs (from the “Billboard
 1494 API” service) under a single high-level code, demonstrating that it learns a true functional hierarchy
 1495 that transcends superficial metadata. Representative tools include:

- 1496 • Hot 100 (from the “Billboard” service)
- 1497 • New Zealand Songs (from the “Billboard API” service)
- 1498 • Billboard Japan Hot 100 (from the “Billboard API” service)
- 1499 • Artist 100 (from the “Billboard” service)

1500 This learned structure provides a robust foundation for complex reasoning. The shared parent code
 1501 <T1_184> acts as a strong collaborative prior, signaling to the model that these distinct chart APIs
 1502 can be orchestrated to fulfill a multifaceted request (e.g., comparing charts across regions). This is
 1503 a clear example of how our collaborative-aware tokenization creates a meaningful structure that is
 1504 essential for enabling complex, multi-step planning.

1512
 1513 **Case 3: Coherent Semantic Grouping for Coordination (<T1_996>).** We further observe that
 1514 <T1_996> successfully aggregates distinct tools related to *Health & Fitness Metrics*. This parent
 1515 code clusters various metabolic calculation tools by function. Representative tools include:

1516 • BMI Calculator v2 (for standard BMI calculation)
 1517 • BMI v2 (handling specific inputs like metric vs. imperial units)
 1518 • BMR & TMR (for metabolic rate calculations)

1521 By organizing these functionally similar but operationally distinct tools under a coherent “Health
 1522 Metrics” family, the model establishes a stable semantic anchor in the latent space. This shared
 1523 parent code serves as a critical navigational aid, allowing the model to effectively pivot between
 1524 related tool variations when specific input requirements (e.g., units of measurement) change during
 1525 a task.

1527 C.1.2 MULTI-TOOL COORDINATION IN TRAJECTORIES

1529 To explicitly demonstrate how the coherent grouping described in **Case 3** facilitates actual task
 1530 execution, Figure 9 presents a real execution trajectory.

1532 In this scenario, the user requests a comprehensive integration guide for a BMI app, requir-
 1533 ing the use of multiple distinct BMI calculators. The trajectory reveals that the model consis-
 1534 tently utilizes tools within the <T1_996> family defined above. It first invokes the standard
 1535 BMI tool (<T1_996><T2_258>). Realizing the need for versatile inputs, it seamlessly piv-
 1536 ots to a metric-specific endpoint (<T1_996><T2_606>) and then to an imperial-unit endpoint
 1537 (<T1_996><T2_328>). This behavior demonstrates that the shared parent code acts as a collab-
 1538 orative bridge, allowing the model to effectively “explore” related sub-functions (the child codes)
 1539 without losing the high-level context of the task.

1541 C.2 EXAMPLES FOR TOOLS AND APIs

1543 To illustrate the diversity and realism of the tools and APIs used in our experiments, we present
 1544 two representative examples from the ToolBench dataset. As shown in Figure 6, the first example
 1545 demonstrates a real-world RESTful API for extracting information from a Thai driver’s license, in-
 1546 cluding its endpoint, required parameters, and a sample implementation snippet. Figure 7 showcases
 1547 a functional tool that converts URLs into QR code images, highlighting its usage description, sup-
 1548 ported parameters, and implementation code. These examples reflect the practical and executable
 1549 nature of the APIs included in ToolBench.

1551 C.3 EXAMPLES OF ALIGNMENT TUNING DATA

1553 We also present examples for our two-stage generative alignment process. Figure 10 shows a training
 1554 instance for tool retrieval alignment, where the model learns to generate a tool’s symbolic identifier
 1555 from a query. Figure 11 demonstrates a training instance for tool usage trajectory alignment. It
 1556 shows a multi-step interaction where the agent reasons, invokes tools, and recovers from failures to
 1557 complete the task.

1559 C.4 REAL END-TO-END INFERENCE TRAJECTORY

1561 To further illustrate how ToolWeaver behaves at inference time, Figure 12 presents a real end-to-
 1562 end tool-use trajectory on a complex, multi-part ToolBench-style query. The user asks the agent to
 1563 design a treasure hunt game that uses QR codes embedding riddles, per-clue identifiers, and a global
 1564 UUID for the entire game session. For clarity, we omit the verbose system prompt and only show
 1565 the user and assistant turns, as well as the intermediate action and argument tokens generated by the
 1566 model.

1566	Multi-Tool Coordination Trajectory (BMI Integration Task)	
1567	User Query I'm designing a mobile app for tracking body mass index, and I need to integrate the BMI calculation API. Could you provide me with the necessary API endpoints and parameters?	
Step 1: Retrieve Standard Calculator		
1572	Thought The user needs BMI endpoints. I will start by retrieving the standard calculator to cover the basic use case.	
1574	Action Tool: bmi_for_bmi_calculator_v2 Code: <T1_996><T2_258> (Family: Health Metrics) Args: {"weight": 70, "height": 170}	
Step 2: Explore Metric-Specific Variation		
1579	Thought To provide a comprehensive guide, I should also check for endpoints that specifically accept explicit metric units to ensure precision.	
1581	Action Tool: gives_the_bmi_when_you_input_values_in_metric_units Code: <T1_996><T2_606> (Same Parent Code) Args: {"heightincm": 170, "weightinkg": 70}	
Step 3: Explore Imperial-Unit Variation		
1586	Thought Finally, I need to cover users who prefer imperial units (feet and inches) to make the app integration guide complete.	
1588	Action Tool: height_in_feet_and_inches_input_weight_in_kilograms Code: <T1_996><T2_328> (Same Parent Code) Args: {"weightinkg": 70, "heightfeet": 5, "heightinches": 10}	
1593	Answer Here are the necessary API endpoints for your BMI app: 1. Standard: bmi... 2. Metric: gives_the_bmi... 3. Imperial: height_in_feet...	

Figure 9: A real execution trajectory demonstrating intra-family coordination. The model leverages the shared parent code <T1_996> (Health Metrics) to coherently navigate between three distinct but functionally related BMI tools (Standard, Metric, Imperial) to fulfill a complex user request.

1598	Retrieval Training
1599	User:
1600	My friend is a big fan of TV shows and wants to know the most popular TV shows right now. Can you fetch the list of most popular TV shows? Also, provide the overview details of these shows, such as their running time and number of episodes.
1603	Assistant:
1604	{Tool Identifier for "Title Get Overview Details"}
1605	

Figure 10: Dataset example for tool selection in retrieval training. We use user role to represent queries and assistant role to represent the chosen tool invocation. The placeholder {Tool Identifier ...} represents the target output, whose format varies depending on the specific tokenization method being trained.

D THE USAGE OF LLMs

LLMs were used as an assistive tool to improve the grammar and clarity of the manuscript, help summarize related literature, and refine concepts for figures. The core research ideas, experimental design, and conclusions were developed entirely by the human authors, who take full responsibility for the final content of this paper.

1620
1621
1622
1623
1624
1625
1626
1627

End-to-End Agent-Tuning	
1628	System: You are AutoGPT, you can use many tools (functions) to do the following task. First I will give you the task description, and your task start. At each step, you need to give your thought to analyze the status now and what to do next, with a function call to actually execute your step. After the call, you will get the call result, and you are now in a new state. Then you will analyze your status now, then decide what to do next... After many (Thought-call) pairs, you finally perform the task, then you can give your final answer. Remember: 1. The state change is irreversible, you can't go back to one of the former states. If you want to restart the task, say "I give up and restart". 2. All the thought is short, at most in 5 sentences. 3. You can do more than one try, so if your plan is to continuously try some conditions, you can do one of the conditions per try. Let's Begin! Task description: You should use functions to help handle the real time user queries. Remember: 1. ALWAYS call Finish function at the end of the task. And the final answer should contain enough information to show to the user. If you can't handle the task, or you find that function calls always fail (the function is not valid now), use function Finish->give.up.and.restart. 2. Only generate actions and inputs.
1642	User: Are you able to help me sanitize some text that has profanity? I'm looking for a way to automatically remove any bad words. Can you clean up this sentence - 'this is some damn good text that needs cleaning. Clearly its pretty crap.'? Begin!
1645	User: This is not the first time you try this task, all previous trials failed. Before you generate my thought for this state, I will first show you your previous actions for this state, and then you must generate actions that is different from all of them. Here are some previous actions candidates: [{"name": "Tool Identifier for Remove Profanity", "arguments": "\n\\\"text\\\": \\"this is some damn good text that needs cleaning. Clearly its pretty crap.\\"", "function_output": "\\\"error\\\": \\"", "response": "\\\"message\\\": \\"API doesn't exists\\\""}] Remember you are now in the intermediate state of a trial, you will first analyze the now state and previous action candidates, then make actions that is different from all the previous.
1652	Assistant: Based on the previous action, it seems that the function call to {Tool Identifier for Remove Profanity} failed because the API does not exist. To handle the profanity in the text, I will use a different approach. Instead of relying on an external API, I will manually create a list of profanity words and replace them with asterisks. My new action will be to replace the profanity words in the text with asterisks.
1656	User: Generate the action. Assistant: <>Finish>>
1657	User: Please give the input. Here is the documentation: {'required': [], 'optional': [{'name': 'give_answer', 'description': 'Output the answer', 'type': 'string', 'name': 'give.up.and.restart', 'description': 'Unable to handle the task from this step', 'type': 'string'}]}
1660	Assistant: { "return_type": "give_answer", "final_answer": "this is some **** good text that needs cleaning. Clearly its pretty ****."}

1664 Figure 11: An example for end-to-end agent-tuning. The placeholder {Tool Identifier
1665 ... } represents the target output, whose format varies depending on the specific tokenization
1666 method being trained.
1667
1668
1669
1670
1671
1672
1673

1674

1675

1676

1677

1678

1679

1680

1681

1682

1683

1684

1685

1686

1687

1688

1689

1690

1691

1692

1693

1694

1695

1696

1697

1698

1699

1700

1701

1702

1703

1704

1705

1706

1707

1708

1709

1710

1711

1712

1713

1714

1715

1716

1717

1718

1719

1720

1721

1722

1723

1724

1725

1726

1727

End-to-End Tool-Use Trajectory	
System:	Standard AutoGPT-style tool-using instructions (omitted here for brevity).
User:	I am planning a treasure hunt game for my family reunion and I want to use QR codes to provide clues. Generate QR codes with riddles as the data parameter for each clue. Additionally, include a random string of characters as a unique identifier for each QR code. Finally, generate a UUID for the treasure hunt game to ensure the uniqueness of the game session.
Assistant:	To generate QR codes with riddles as the data parameter for each clue, I first decide to call the "<T1.124><T2.781>" function, which corresponds to the qr_code_gen_for_qr_api tool. This tool converts a URL into a QR code image, and I will use it to quickly verify that I can generate a basic QR code for one of the clues.
User:	Generate the action.
Assistant:	qr_code_gen_for_qr_api
User:	Please give the input. Here is the documentation: <code>{"name": "QR Code API (Web URL)", "description": "Call the API Endpoint /qr and pass in the url parameter...", "required": [{"name": "url", "type": "STRING"}], "optional": [...]}</code>
Assistant:	<code>{"url": "https://example.com/clue1"}</code>
Assistant:	The basic URL-to-QR API works, but it only accepts a simple URL string and cannot directly encode richer structured data such as "riddle text + per-clue identifier". To embed both the riddle and a random string in the QR payload, I need a more flexible QR code generator that allows arbitrary data content and styling. For this, I will use the "<T1.93><T2.913>" function.
User:	Generate the action.
Assistant:	create_qr_code_for_flowcode
User:	Please give the input. Here is the documentation: <code>{"name": "Generate Advance - Direct Image", "description": "Generates a QR code as a direct image with additional settings.", "required": [{"name": "data", "type": "STRING"}], "optional": [...]}</code>
Assistant:	<code>{"data": "GameSession: FAMILY-REUNION-2025; ClueId: Z7QK9M; Riddle: What is the capital city of France?", "imageType": "png", "style": "default", "moduleShape": "circle", "rimTextTop": "Clue 1", "rimTextBottom": "Scan to reveal the riddle!"}</code>
Assistant:	To generate a UUID for the overall treasure hunt game session (distinct from the per-clue random string embedded in each QR code), I now need to call the "<T1.621><T2.2>" function. This corresponds to the random_uuid_for_teamriverbubbles_random_utilities tool, which returns a UUID v4 that I can use as a unique game identifier.
User:	Generate the action.
Assistant:	random_uuid_for_teamriverbubbles_random_utilities
User:	Please give the input. Here is the documentation: <code>{"name": "Generate UUID", "description": "Generate UUID v4 with dash or not.", "required": [], "optional": [...]}</code>
Assistant:	<code>{}</code>
Assistant:	The UUID tool has returned a unique identifier for the treasure hunt game session, which I will associate with all generated QR codes. Each QR code embeds its own ClueId (e.g., Z7QK9M) inside the data field, while the session-level UUID serves as a global game identifier for tracking and management.
User:	Generate the action.
Assistant:	<<Finish>>
User:	Please give the input. Here is the documentation: <code>{"required": [], "optional": [{"name": "give_answer", "description": "Output the answer", "type": "string"}, {"name": "give_up_and_restart", "description": "Unable to handle the task from this step", "type": "string"}]}</code>
Assistant:	<pre>{ "return_type": "give_answer", "final_answer": "I have generated a treasure-hunt QR code clue that embeds both a riddle and a per-clue identifier, and also created a UUID for the whole game session. Concretely, the advanced QR API is called with a data payload like 'GameSession: FAMILY-REUNION-2025; ClueId: Z7QK9M; Riddle: What is the capital city of France?', and rendered as a PNG image with circular modules, top rim text 'Clue 1', and bottom rim text 'Scan to reveal the riddle!'. Separately, the UUID tool returns a game-level identifier such as 'e286537a-2758-4144-8890-22a575b9157a', which uniquely tags this treasure hunt session." }</pre>

Figure 12: A real end-to-end inference trajectory of ToolWeaver handling a complex, multi-part user query. The system prompt is omitted for brevity. The agent successfully reasons, selects multiple tools via hierarchical codes, adapts its tool choice after an initial limitation, and synthesizes the final answer.